Engineered E. coli for the targeted deposition of therapeutic payloads to sites of disease

Jason Lynch
Massachusetts General Hospital
Coral Coral González-Prieto
Massachusetts General Hospital
Analise Reeves
Synlogic
Urmila Powale
Tufts University
Neha Godbole
Massachusetts General Hospital
Jacqueline Tremblay
Tufts Cummings School of Veterinary
Florian Schmidt
University of Bonn https://orcid.org/0000-0002-9979-9769
Hidde Ploegh
Boston Children's Hospital https://orcid.org/0000-0002-1090-6071
Jonathan Glickman
Beth Israel Deaconess Medical Center
John Leong
Tufts University
Charles Shoemaker
Tufts Cummings School of Veterinary
Wendy Garrett
Harvard University https://orcid.org/0000-0002-5092-0150
CAMMIE LESSER (clesser@mgh.harvard.edu)
Massachusetts General Hospital

Article

Keywords:

Posted Date: January 21st, 2022

DOI: https://doi.org/10.21203/rs.3.rs-1233122/v1

Engineered *E. coli* for the targeted deposition of therapeutic payloads to sites of disease

#Jason P. Lynch[1,2], #Coral González-Prieto[1,2], Analise Z. Reeves[1,2], Urmila Powale[1,2], Neha Godbole[1,2], Jacqueline M. Tremblay[3], Florian I. Schmidt[4], Hidde L. Ploegh[5], Jonathan N. Glickman[6,7], John M. Leong[8], Charles B. Shoemaker[3], Wendy S. Garrett[9,10,11], *Cammie F. Lesser[1,2,11]

[1]Center for Bacterial Pathogenesis, Division of Infectious Diseases, Department of Medicine, Massachusetts General Hospital, MA 02115, USA.

[2]Department of Microbiology, Blavatnik Institute, Harvard Medical School, Boston, MA 02115, USA.

[3]Department of Infectious Disease and Global Health, Tufts Cummings School of Veterinary Medicine, North Grafton, Massachusetts, MA 01536, USA

[4]Institute of Innate Immunity, Medical Faculty, University of Bonn, 53127 Bonn, Germany.

[5]Boston Children's Hospital and Harvard Medical School, Boston, MA 02115, USA

[6]Department of Pathology, Harvard Medical School, Boston, MA 02115, USA.

[7]Beth Israel Deaconess Medical Center, Boston, MA 02215-5400, USA.

[8]Department of Molecular Biology and Microbiology, Tufts University School of Medicine, Boston, MA, 02111, USA.

[9]Departments of Immunology and Infectious Diseases and Harvard T. H. Chan Center for the Microbiome in Public Health, Harvard T.H. Chan School of Public Health, Boston, MA 02115, USA.

[10]Department of Medical Oncology, Dana-Farber Cancer Institute, Boston, MA 02215, USA.

[11]Broad Institute of MIT and Harvard, Cambridge, MA 02142, USA.

[#]These authors contributed equally

*Correspondence: clesser@mgh.harvard.edu (C.F. Lesser)

Abstract

New drug platforms are needed which enable the directed delivery of therapeutics to sites of disease to maximize efficacy and limit off-target effects. Here, we report the development of $PROT_3EcT$, commensal *Escherichia coli* engineered for the direct secretion of proteins into their surroundings. $PROT_3EcT$ are composed of four modular components: an *E. coli* chassis, a modified bacterial protein secretion system, a regulatable transcriptional activator, and a secretable therapeutic payload. $PROT_3EcT$ that secrete functional single-domain antibodies, nanobodies (Nb), stably colonize and maintain a functional secretion system within the intestines of mice. A single prophylactic dose of $PROT_3EcT$ that secretes a tumor necrosis factor alpha (TNFα) neutralizing Nb is sufficient to ablate TNF levels and prevent the development of injury and inflammation in a chemically-induced model of inflammatory bowel disease. This work lays the foundation for the development of $PROT_3EcT$ as a therapeutic platform for the treatment of at least gastrointestinal-based diseases.

Introduction

Microbe-based therapeutics are emerging as a platform for the development of interventions for the treatment of a variety of diseases, particularly those with etiologies linked to the gut. In addition to searching for cocktails of beneficial natural isolates, synthetic biology-based approaches are being used to engineer microbes with additional therapeutic capabilities, including the targeted deposition of therapeutic payloads to sites of disease. Due to their ease of production, administration, and natural capacity to synthesize and deliver complex biologics, engineered microorganisms hold enormous potential as affordable options to traditional biologic therapies. In addition, by outfitting them with high specificity payloads, they provide a platform for the development of interventions with improved efficacy and limited off-target effects.

Escherichia coli Nissle 1917 (EcN), a probiotic with GRAS (generally recognized as safe) status[1], is gaining traction as a chassis for synthetic biology. EcN has inherent anti-bacterial and anti-inflammatory activities and is genetically tractable. A variety of strategies are being pursued to enhance its therapeutic potential. For example, variants with enhanced metabolic capabilities are being investigated for removal of toxic intermediates associated with metabolic diseases[2-4]. Similarly, efforts are underway to develop variants that deliver therapeutic payloads to sites of disease. However, given the difficulty with engineering Gram-negative bacteria to secrete proteins into their surroundings, work has primarily focused on developing variants of EcN programmed to release intracellular cargo[5-7] as well as to express outer membrane adhesins[8] and Curli modified to display proteins of interest on the bacterial surface[9].

The general secretion (Sec) and twin arginine translocation (Tat) pathways, common to both Gram-negative and Gram-positive bacteria, are the main systems by which both transport proteins across their cytosolic membranes[9]. These systems promote the deposition of proteins into the surroundings of Gram-positive bacteria, but only into the outer membrane of their Gram-negative relatives. Only a small subset of periplasmic proteins are targeted for secretion across their outer membrane into the surroundings (for review, see[10]). However, numerous Gram-negative bacterial pathogens utilize complex nanomachines, including type III secretions systems (T3SSs), to transport bacterial proteins directly into the cytosol of host cells. The fully assembled type III secretion apparatus (T3SA) is embedded within the outer envelope of the bacterium with a needle-like extension that docks onto and forms pores in host cell membranes. We previously established that the T3SA of *Shigella flexneri* is functional when introduced into laboratory strains of *E. coli*[11-14].

Here, we report the development of PROT$_3$EcT (PRObiotic Type 3 secretion *E. coli* Therapeutic), *E. coli* engineered with a *Shigella* T3SA modified to secrete proteins into its surroundings, as opposed to directly into eukaryotic cells. When fused to an N-terminal type III

secretion sequence, fully functional camelid single-domain antibodies (also known as nanobodies or VHH), are secreted by PROT$_3$EcT. PROT$_3$EcT is modular in design, composed of four elements: (1) an *E. coli* strain, (2) the modified T3SA, (3) its master transcriptional regulator (VirB), and (4) a therapeutic payload (Fig. 1a). PROT$_3$EcT-4, a variant of PROT$_3$EcT engineered such that all components are maintained in the absence of antibiotic selection, is unimpaired in growth and capable of colonizing the intestines of mice for at least 14 days. In support of the therapeutic potential of the PROT$_3$EcT platform, TNF-PROT$_3$EcT, a variant of PROT$_3$EcT-4 engineered to secrete an anti-TNFα nanobody, is as effective as systemically administered anti-TNFα monoclonal antibodies in suppressing the development of inflammation in a chemically induced preclinical model of inflammatory bowel disease. Together, these studies provide the foundation for the further development of PROT$_3$EcT as a versatile therapeutic platform (Fig. 1b).

Results

Development of PROT$_3$EcT

The genes that encode the ~20 components that form the *Shigella* T3SA are contained within the adjacent Ipa, Mxi, and Spa operons on a large virulence plasmid[15, 16]. The Mxi and Spa operons encode all of the structural components needed to form the T3SA. The Ipa operon encodes the proteins that form the tip complex that holds the machine in an OFF configuration prior to host cell contact and a pore complex in the host cell membrane upon which the machine docks before injecting proteins into host cells[17-19]. We previously described a recombineering-based platform to transfer large regions of this virulence plasmid into defined engineered synthetic loci on the *E. coli* chromosome[11-13, 20]. Using this technology, we developed laboratory strains of *E. coli* that encode and express the Ipa, Mxi, and Spa operons capable of delivering heterologous proteins into mammalian cells[14].

With the goal of developing *E. coli* that efficiently secrete proteins into their surroundings (Fig. S1), we compared the secretory activity of DH10b *E. coli* that contain the Ipa, Mxi and Spa operons versus the Mxi and Spa operons, each inserted at a single defined chromosomal locus. Each strain was transformed with a low-copy number plasmid that expresses VirB, the shared transcription factor of the Mxi, Spa and Ipa operons (Fig. S1a), under the control of the IPTG (isopropyl β- d-1-thiogalactopyranoside)-inducible P*trc* promoter. The resulting strains are referred to here as mT3Ec_Ipa-Mxi-Spa and mT3Ec_Mxi-Spa (Fig. S1b).

When grown under conditions that promote T3SA expression and exposed to Congo red, a dye that triggers secretion in the absence of host cells[21], mT3Ec_Ipa-Mxi-Spa and mT3Ec_Mxi-Spa, secreted similar levels of IPTG-inducible OspC2 (a native *Shigella* T3SA secreted protein), demonstrating that the absence of the Ipa operon has no effect on the activity of the T3SA (Fig. 2a). To ensure that OspC2 detected in the supernatant fractions was not due to bacterial cell lysis, we also monitored for the presence of GroEL, a highly abundant cytosolic protein. As expected, GroEL was detected in the intact bacteria, but not in the supernatant factions (Fig. 2a). Furthermore, in the absence of Congo red, OspC2 was abundantly secreted by mT3Ec_Mxi-Spa, but not mT3Ec_Ipa-Mxi-Spa, demonstrating that mT3Ec_Mxi-Spa constitutively secretes proteins into its surroundings (Fig. 2b). When we examined the full set of proteins present in the supernatant of mT3Ec_Mxi-Spa, OspC2 was the most abundantly secreted bacterial protein, establishing that the introduction of the Mxi-Spa operons and VirB is sufficient to outfit DH10b *E. coli* with a robust IPTG-inducible secretion system (Fig. 2c).

We next investigated whether similar modifications to two non-pathogenic human *E. coli* isolates would similarly equip these strains with a functional protein secretion system. First, we developed PROT$_3$EcT-1, *E. coli* Nissle 1917 (EcN) engineered with the Mxi-Spa operons at the analogous chromosomal locus as mT3Ec_Mxi-Spa. To test whether PROT$_3$EcT-1 assembles a functional T3SA, we introduced plasmids encoding IPTG-inducible *virB* and *ospC2* (Fig. 2d) and

monitored OspC2 secretion following induction of expression of both. VirB-expressing PROT$_3$EcT-1, like mT3Ec_Mxi-Spa, secretes OspC2 (Fig. 2e), albeit at somewhat lower levels. Similar modifications to the *E. coli* human isolate HS, led to the generation of PROT$_3$EcT-2, which secreted OspC2 at levels closer to that of mT3Ec_Mxi-Spa (Fig. S1c), suggesting that the Mxi-Spa T3SA platform will function similarly when introduced into additional *E. coli* strains.

To mimic the *in vivo* situation more closely, and to assess whether the strains have extended secretory activity, we followed the levels of OspC2 in the supernatant fractions of mT3Ec_Mxi-Spa and PROT$_3$EcT-1 when grown in media that supports their growth. Increasing levels of secreted OspC2, but not GroEL, was observed over a 6-hour time course (Fig. 2f).

Lastly, *Shigella* are intracellular pathogens that rely on their T3SS and its secreted proteins to invade non-phagocytic epithelial cells. Given that bacteria engineered with the Mxi-Spa operons lack effectors, they are not expected to invade host cells. We therefore compared the ability of *Shigella,* PROT$_3$EcT-1, mT3Ec_Mx-Spa, DH10b *E. coli* and EcN to invade cells using a gentamicin protection assay. As expected, *Shigella*, but none of the other strain were observed within epithelial cells (Fig. 2g).

PROT$_3$EcT can be engineered to secrete nanobodies

Nanobodies (Nb), the ~15kDa variable domains of heavy chain-only antibodies, are ideal substrates from our bacterial secretion system as they are small stable proteins that generally exhibit strong antigen-binding affinity. We previously found that fusion of the first ~50 N-terminal amino acids of numerous *Shigella* type III effectors to heterologous proteins is sufficient to generate variants secreted by mT3Ec_Ipa-Mxi-Spa[12, 14]. Thus, we screened for modifications to a representative Nb that result in its recognition by PROT$_3$EcT. Nb$^{ASC\ 22}$ was fused to the first 50 residues of eight *Shigella* effectors (IpaH4.5, IpaH7.8, IpaH9.8, OspE, OspF, OspD3, VirA, and OspG). We hereafter refer to these regions as secretion sequences. Nb^{ASC} fused to the OspC2

or OspG secretion sequences resulted in the highest level of secretion (Fig. 3a). Fusion of the OspC2 secretion sequence also resulted in secretion of monomeric $Nb^{PD\text{-}L1}$ [23], Nb^{CTLA4} [24], Nb^{NPI} [25], and Nb^{Stx2} [26] as well as heterodimeric and heterotrimeric Nb^{Stx2} (Fig. 3b, c). As observed with OspC2 (Fig. 2c), Nbs were the most abundant protein present in the supernatants of $PROT_3EcT$-1 (Fig. 3d).

In parallel, we investigated whether some of the native *E. coli* secretion systems that are currently explored for secretion of recombinant proteins[27-30] can also be adapted to secrete Nbs. In these systems, the proteins are secreted via a 2-step process. Post-delivery into the periplasm via the Sec system, they are secreted across the outer membrane via unknown pathway(s). We fused Nb^{Stx2} to full length *E. coli* OsmY, *E. coli* YebF and *Bacillus* Cel-CD, as well as the first 20 residues of Cel-CD, which encodes its secretion signal sequence. Only fusion to YebF resulted in a secreted Nb, which was present at much lower levels in the supernatants of EcN as compared to the same Nb in the supernatants of $PROT_3EcT$ (Fig. S2a). We were unable to detect expression of the Cel-CD fusions, which reflected a lack of expression rather than a deficiency of our detection method because the expression and secretion of Cel-CD fusion proteins was detectable when expressed in protease-deficient BL21 *E. coli* (Fig. S2b), consistent with published studies[29, 30]. Thus, at least for the candidate Nb studied, the $PROT_3EcT$ platform vastly outperformed the native *E. coli* secretion systems.

Development of constitutively active Nb-secreting $PROT_3EcT$

Before studying $PROT_3EcT$ in mouse models of disease, we sought to generate a variant that constitutively secretes Nbs and maintains all its genetically engineered components in the absence of antibiotic selection. For VirB, we first replaced its IPTG-inducible P*trc* promoter with ones predicted to be constitutively active in the gut, *Shigella* P*virF* [31], *E. coli* P*ompC* [32], and two synthetic promoters, BBa_J23115 and BBa_J23119[33]. $PROT_3EcT$-1 variants

carrying plasmids that encode each of these constitutively active VirB secreted Nbs at levels as the variant expressing IPTG-inducible VirB (Fig. 4a). Thus, we introduced the P*J23119-virB* expression cassette into the chromosome of PROT$_3$EcT-1. The resulting strain, PROT$_3$EcT-3 (Fig. 4b), secreted Nb at levels equivalent to that of the parent strain that encodes P*J23119-virB* on a plasmid (Fig. 4c).

For the Nb expression cassette, we generated a variant that was constitutively expressed by replacing its P*trc* promoter with the constitutive BBa_P*J23108* promoter (Fig. 4d). To maintain flexibility in terms of introducing payload expression circuits and to enable higher levels of expression, rather than introduce these circuits onto the chromosome of PROT$_3$EcT, we chose to encode them on a plasmid. To ensure plasmid maintenance in the absence of antibiotic pressure, we built on prior work from Hwang and colleagues[34] and developed PROT$_3$EcT-4, a derivative that lacks *alr* and *dadX* (Fig 4e). These genes encode EcN's two alanine racemases that convert L- to D-alanine, an amino acid that is essential for cell wall biosynthesis that is very limited in the mammalian GI tract[35]. We then inserted an intact *alr* gene onto the Nb-producing plasmid to facilitate *in vivo* pressure for plasmid maintenance. PROT$_3$EcT-3 and PROT$_3$EcT-4 that carry this plasmid secreted similar levels of Nbs, but whereas Nb-production by PROT$_3$EcT-3 is lost in the absence of antibiotic selection, PROT$_3$EcT-4 stably maintains production (Fig. 4f, Fig. S3a). PROT$_3$EcT-4 and unmodified EcN exhibited essentially identical growth patterns, regardless of whether the bacteria expressed and secreted Nbs (Fig. 4g), indicating that these modifications do not add a significant metabolic burden.

PROT$_3$EcT stably colonizes the gastrointestinal tract of mice.

Our initial *in vivo* experiments focused on investigating the ability of Nb-secreting PROT$_3$EcT-4 to colonize the mouse gastrointestinal tract while maintaining a functional

200 secretion system. We first monitored the levels of bacteria shed in the feces of mice orally
201 inoculated with EcN or PROT$_3$EcT-4 (Fig. 5a). After the administration of a single dose of ~10^8
202 colony forming units (CFU) via oral gavage, EcN and PROT$_3$EcT-4 were each detected in the
203 shed feces at ~10^5 CFU/gm/day for at least 14 days, with no significant decrease in fecal
204 shedding over that period (Fig. 5b). Each of the 158 Nb-secreting PROT$_3$EcT-4 colonies isolated
205 from a total of 4 mice at 2-, 5-, and 14-days post-inoculation secreted Nbs, indicating that their
206 T3SA remained fully functional and that the *alr*-Nb-expressing plasmid was maintained (Fig. 5c
207 and Fig. S4a-c). No significant weight loss was observed over the course of these experiments
208 (Fig. S4d).

209 Next, we examined the biogeography of PROT$_3$EcT-3 and EcN within the intestines of
210 mice inoculated with variants of each that constitutively express the luciferase-producing
211 *luxCDABE* operon[36]. The two strains exhibited equivalent luciferase activity when grown *in vitro*
212 (Fig. S5a-b). Eight days post-oral inoculation of the mice, each strain exhibited similar patterns
213 of luciferase expression in explanted sections of their ileum, cecum, and proximal colon (Fig.
214 5d). In complementary studies, CFUs of PROT$_3$EcT-3 and EcN found in various regions of the
215 intestines of orally inoculated mice were equivalent and exceeded 5 x 10^9 CFU/g of contents
216 (Fig. S5c).

217 To confirm that the modified T3SS present in PROT$_3$EcT is actively transcribed within
218 the intestines of mice, we developed a *luxCDABE*-based reporter that is only activated when the
219 Mxi-Spa operons, which encode the modified T3SA, are transcribed (Fig. S5d). Variants of
220 PROT$_3$EcT-3, but not EcN, that contained this reporter demonstrated luciferase production *in*
221 *vitro* (Fig. S5e-f) and within the explanted cecum, proximal colon, and ileum of inoculated mice
222 (Fig. 5e). These observations establish that the T3SS present within PROT$_3$EcT-3 is expressed
223 within the intestines of mice and does not interfere with EcN colonization.

PROT$_3$EcT can be engineered to secreted functional Nb^{TNF}

To establish the use of PROT$_3$EcT as a therapeutic platform, we focused efforts on investigating its efficacy in the treatment of inflammatory bowel diseases (IBD). The etiologies of ulcerative colitis and Crohn's disease, collectively termed IBD, are complex and thought to be driven by host genetic, environmental, and microbiota factors. Yet, both diseases exhibit chronic inflammation accompanied by increased levels of pro-inflammatory cytokines[37]. Monoclonal antibodies (mAb) that target the pro-inflammatory cytokine TNFα, e.g., infliximab and adalimumab, are highly efficacious in controlling severe disease and in improving the quality of life of patients with IBD[38]. However, given the systemic administration of these therapeutics, patients receiving these agents are immunosuppressed and at increased risk of developing life-threatening infections and lymphoma[39].

We hypothesized that the targeted delivery of anti-TNFα Nbs via PROT$_3$EcT to the intestines could reduce intestinal inflammation. To investigate this possibility, we first isolated anti-TNFα Nbs from alpacas immunized with recombinant mouse TNFα, including one that binds with high affinity (EC_{50} 0.1 nM) and neutralizes TNFα (IC_{50} 0.1 nM) (Table S1 and Figure S6). We generated both monomeric and dimeric variants of Nbs engineered with an OspC2 secretion sequence. The dimer was secreted much more efficiently than the monomer (Fig. 6a) and PROT$_3$EcT secreted dimeric Nbs were as effective as *E. coli*-purified dimeric Nbs in blocking TNFα-induced death of mouse L929 cells (Fig. 6b).

TNF-PROT$_3$EcT inhibits the development of disease in a mouse model of colitis.

To investigate the utility of PROT$_3$EcT as a live biotherapeutic for the treatment of intestinal inflammation, we interrogated the therapeutic efficacy of TNF-PROT$_3$EcT-4 (PROT$_3$EcT that constitutively secrete the anti-TNF dimeric Nb) in the suppression of TNBS (2,4,6-trinitrobenzene sulfonic acid)-induced colitis. In this preclinical model of IBD, a mixture of

248 TNBS, a hapten, and ethanol, which disrupts the mucosal barrier, is instilled into the colon via
249 rectal administration. TNBS bound to colonic tissue proteins subsequently induces inflammation
250 driven by pro-inflammatory cytokines, including TNFα[40]. As previously reported[41], mice treated
251 intraperitoneally with a neutralizing anti-TNF monoclonal antibody (1-day prior and 2- and 4-
252 days post-administration of TNBS) were protected from weight loss, colon shortening, and
253 histologic evidence of colitis (Fig. S7).

254 To test the therapeutic efficacy of TNF-PROT$_3$EcT, we orally administered 10^8 CFU of
255 TNF-PROT$_3$EcT-4, PROT$_3$EcT-4, or PBS to mice one day before as well as two and four days
256 after they received TNBS (Fig. 6c). Animals that received bacteria shed equivalent levels of 10^5-
257 10^6 CFU/g of TNF-PROT$_3$EcT-4 and PROT$_3$EcT-4 in their feces (Fig. 6d). Treatment with TNF-
258 PROT$_3$EcT-4 significantly reduced weight loss, blunted colon shortening, and decreased or
259 completely abrogated epithelial injury and inflammation in the mucosa, including less
260 polymorphonuclear and mononuclear cell infiltration (Fig. 6e-h). In contrast, PROT$_3$EcT-4 did
261 not provide any protection as assessed by each of these metrics, demonstrating that the
262 therapeutic efficacy afforded by TNF-PROT$_3$EcT is due to the secreted TNF-neutralizing Nb and
263 not EcN intrinsic.

264 Given that enemas are commonly used for drug delivery for patients with IBD, we also
265 investigated the efficacy of intrarectally delivered TNF-PROT$_3$EcT-4 in limiting TNBS-induced
266 colitis using the same dosing strategy as described above (Fig. S8a). As with oral delivery,
267 intrarectally delivered TNF-PROT$_3$EcT-4, but not PROT$_3$EcT-4, ameliorated weight loss, colon
268 shortening, and colitis (Fig. S8b-e). Thus, when delivered either orally or intrarectally, TNF-
269 PROT$_3$EcT-4 provides protection against TNFα-driven inflammation in the TNBS model of
270 colitis.

Therapeutic strains that cannot compete for and establish a replicative niche within the colon may be useful if administered repeatedly to patients. To assess whether treatment with similarly engineered DH10b *E. coli* also suppresses colonic inflammation, we developed T_3EcT, a variant of mT3Ec-Mxi-Spa engineered with the chromosomally encoded P*J23119* VirB gene cassette, and a variant of T_3EcT that secretes Nb^{TNF}, TNF-T_3EcT. After establishing that TNF-T_3EcT constitutively secreted Nb^{TNF} into its surroundings (Fig. S8f), TNF-T_3EcT and T_3EcT were administered orally or intrarectally to mice using the strategy outline above (Fig. S8a). Orally administered TNF-T_3EcT provided no protection, likely due to its inability to colonize the intestines as assessed by fecal shedding (Fig. S8b). In contrast, treatment with rectally delivered TNF-T_3EcT, but not T_3EcT, suppressed colitis (Fig. S8-c-e), likely reflecting repeated transient deposition of anti-TNF Nbs in the colon. These observations demonstrate that the Ipa-Mxi secretion-based platform can be extended to additional *E. coli* strains.

To address whether bacterial secreted Nbs are restricted to the gut, we measured Nb levels in the colonic contents, colon tissue homogenates, and serum of mice treated with each strain across each of the TNBS experiments. To measure the anti-TNF Nb, we used a direct ELISA, which is also capable of detecting the anti-TNF mAb. In mice administered the anti-TNF mAb via an intraperitoneal route, we detected mAb in the serum of 50% of the mice (Fig. S9a). By contrast, levels of serum anti-TNF Nb were below the level of detection in all mice orally inoculated with TNF-PROT$_3$EcT, and only detectable in 20% of mice treated with TNF-PROT$_3$EcT or TNF-T_3EcT via enema. We did not detect evidence of anti-TNF Nbs in the colonic contents or homogenates (Fig. S9b-c).

A single dose of TNF-PROT$_3$EcT is associated with TNFα suppression and inhibition of intestinal inflammation.

Given that the TNF-PROT$_3$EcT-4 treated mice exhibited minimal weight-loss post-administration of TNBS, we tested whether pretreatment with a single dose is therapeutically efficacious. Two days post-TNBS administration, mice pre-treated with a single oral dose of TNF-PROT$_3$EcT-4 (Fig. 6i) exhibited minimal evidence of weight loss, colon shortening, and colitis (Fig. 6k-m). PROT$_3$EcT-4 or the vehicle diluent (PBS) had no effect. As before, similar levels of both strains were shed in the feces (Fig. 6j) and all colonies of shed TNF-PROT$_3$EcT-4 retained the ability to secrete anti-TNF Nb (Fig S7f). For these experiments, mice were sacrificed two days post-administration of TNBS, a time point at which we reproducibly detected elevated proinflammatory cytokine levels within colonic tissue in controls. Significantly lower levels of TNFα and IL-6 were detectable within the colonic tissue of mice pretreated with TNF-PROT$_3$EcT-4 (Fig. 6n-o), suggesting that the secreted anti-TNFα Nb sequesters its target and reduces IL-6. While others have observed that TNF neutralization or EcN treatment can increase IL-10 production in the gut, we observed equivalent levels of IL-10, regardless of the intervention (Fig. 6p).

Discussion

Here we describe the development of PROT$_3$EcT, *E. coli* engineered for the *in-situ* delivery of high specificity protein payloads to sites of disease. Using synthetic biology-based approaches we have engineered both laboratory and non-pathogenic human *E. coli* isolates with a T3SA modified to secrete proteins in a regulated or constitutive manner. PROT$_3$EcT engineered with a constitutively active secretion system that is maintained in the absence of antibiotic selection exhibited growth *in vitro* at rates equivalent to unmodified EcN and can colonize the intestines of mice for at least 14 days.

We demonstrate the ability of TNF-PROT$_3$EcT, a variant that constitutively secretes anti-TNF Nbs, to suppress the development of inflammation in a preclinical mouse model of IBD. Orally or rectally administered TNF-PROT$_3$EcT was as efficacious as systemically administered

anti-TNF mAb in limiting the development of TNBS-induced colitis. Other groups have also engineered microbes to treat gut inflammation, the most closely related being variants of *Lactococcus lactis* that secrete IL-10, an anti-inflammatory cytokine, or an anti-TNF Nb[42, 43]. A native secretion system of this Gram-positive bacterium was repurposed for the secretion of therapeutic payloads. However, the strain of *L. lactis* used does not colonize the intestines of humans or mice[44, 45] and may vary in its metabolic activity within the mammalian intestine[46], likely accounting for why it only moderately suppressed inflammation when administered on a daily basis. By contrast, we observe that pre-treatment with just a single oral dose of TNF-$PROT_3EcT$ significantly ameliorates colonic inflammation and injury.

The modular design of $PROT_3EcT$ is such that it can be adapted to secrete different payloads as well as to respond to environmental cues. For example, in future studies, by altering the conditions that induce expression of VirB, $PROT_3EcT$'s T3SA could be endowed with an 'on switch' triggered by specific signals of the gut's inflammatory milieu, *e.g.*, reactive nitrogen species[36, 47-49]. In terms of therapeutic payloads, we demonstrate the versatility of $PROT_3EcT$ to secrete different Nbs, including Nbs that inhibit the activity of bacterial toxins (Nb^{Stx2}) or immune checkpoint molecules ($Nb^{PD\text{-}L1}$ and $Nb^{CTLA\text{-}4}$). While the Nbs we studied were each derived from immunized alpacas, synthetic yeast- and bacterial-based Nb libraries are also available that can be screened rapidly for Nbs with desired properties[50, 51]. Furthermore, $PROT_3EcT$ is not limited to the secretion of Nbs, as we and others have previously established that a variety of other heterologous proteins can be recognized as type III secreted substrates[52]. By altering its route of administration, $PROT_3EcT$ can be expanded for the deposition of therapeutics not only to the gastrointestinal tract, but also to solid tumors, as EcN home to and colonize a variety of solid tumors when administered intravenously, at least in mice[53].

Given its inherent anti-inflammatory and anti-microbial properties, EcN is GRAS and has been used for over a century to treat various intestinal diseases and is available over-the-counter in some countries. However, EcN contains an operon that mediates the synthesis of a

colibactin, a genotoxin capable of mediating the formation of DNA crosslinks[54]. Other colibactin-producing *E. coli* promote the development of colorectal cancer (CRC) in mouse models[55] and induce mutational signatures found in human CRC[56]. Whether this will turn out to be an issue that limits the use of EcN-based therapeutics in humans remains to be discovered. However, EcN mutants deficient in colibactin biosynthesis are not impaired in their ability to colonize the intestines of at least mice[57, 58]. In future studies, we intend to test the ability of colibactin-deficient EcN-based TNF-PROT$_3$EcT to suppress intestinal inflammation. Herein, we found that two colibactin-negative strains, *E. coli* HS and DH10ß[59], can also be engineered with a functional secretion system. While the anti-TNF Nb-secreting, *E. coli* DH10ß based, mT3Ec_Mxi-Spa, was unable to colonize the intestines, rectally administered mT3Ec_Mxi-Spa suppressed TNBS-induced inflammation as efficacious as EcN-based TNF-PROT$_3$ECT.

In summary, we describe the development and characterization of PROT$_3$EcT, programmable *E. coli* engineered for the site-specific delivery of therapeutic payloads to sites of disease. While the presented studies support the further development of PROT$_3$EcT for the treatment of IBD, its modularity permits its rapid adaptation into a therapeutic platform for a broad range of diseases.

References

1. Sonnenborn, U. & Schulze, J. The non-pathogenicEscherichia colistrain Nissle 1917 – features of a versatile probiotic. *Microbial Ecology in Health and Disease* **21**, 122-158 (2009).
2. Kurtz, C.B. et al. An engineered E. coli Nissle improves hyperammonemia and survival in mice and shows dose-dependent exposure in healthy humans. *Sci Transl Med* **11**, eaau7975 (2019).
3. Isabella, V.M. et al. Development of a synthetic live bacterial therapeutic for the human metabolic disease phenylketonuria. *Nat Biotechnol* **36**, 857-864 (2018).
4. Crook, N. et al. Adaptive Strategies of the Candidate Probiotic E. coli Nissle in the Mammalian Gut. *Cell Host Microbe* **25**, 499-512 e498 (2019).
5. Danino, T. et al. Programmable probiotics for detection of cancer in urine. *Sci Transl Med* **7**, 289ra284 (2015).

6. Din, M.O. et al. Synchronized cycles of bacterial lysis for in vivo delivery. *Nature* **536**, 81-85 (2016).
7. Gurbatri, C.R. et al. Engineered probiotics for local tumor delivery of checkpoint blockade nanobodies. *Sci Transl Med* **12** (2020).
8. Piñero-Lambea, C. et al. Programming Controlled Adhesion of E. coli to Target Surfaces, Cells, and Tumors with Synthetic Adhesins. *ACS Synthetic Biology* **4**, 463-473 (2015).
9. Praveschotinunt, P. et al. Engineered E. coli Nissle 1917 for the delivery of matrix-tethered therapeutic domains to the gut. *Nat Commun* **10**, 5580 (2019).
10. Dalbey, R.E. & Kuhn, A. Protein Traffic in Gram-negative bacteria – how exported and secreted proteins find their way. *FEMS Microbiology Reviews* **36**, 1023-1045 (2012).
11. Du, J. et al. The type III secretion system apparatus determines the intracellular niche of bacterial pathogens. *Proc Natl Acad Sci U S A* **113**, 4794-4799 (2016).
12. Ernst, N.H., Reeves, A.Z., Ramseyer, J.E. & Lesser, C.F. High-Throughput Screening of Type III Secretion Determinants Reveals a Major Chaperone-Independent Pathway. *mBio* **9** (2018).
13. Mou, X., Souter, S., Du, J., Reeves, A.Z. & Lesser, C.F. Synthetic bottom-up approach reveals the complex interplay of Shigella effectors in regulation of epithelial cell death. *Proc Natl Acad Sci U S A* **115**, 6452-6457 (2018).
14. Reeves, A.Z. et al. Engineering Escherichia coli into a protein delivery system for mammalian cells. *ACS Synth Biol* **4**, 644-654 (2015).
15. Buchrieser, C. et al. The virulence plasmid pWR100 and the repertoire of proteins secreted by the type III secretion apparatus of Shigella flexneri. *Mol Microbiol* **38**, 760-771 (2000).
16. Venkatesan, M.M. et al. Complete DNA sequence and analysis of the large virulence plasmid of Shigella flexneri. *Infect Immun* **69**, 3271-3285 (2001).
17. Sasakawa, C. et al. Functional organization and nucleotide sequence of virulence Region-2 on the large virulence plasmid in Shigella flexneri 2a. *Molecular Microbiology* **3**, 1191-1201 (1989).
18. Ménard, R., Sansonetti, P., Parsot, C. & Vasselon, T. Extracellular association and cytoplasmic partitioning of the IpaB and IpaC invasins of S. flexneri. *Cell* **79**, 515-525 (1994).
19. Ménard, R., Prévost, M.C., Gounon, P., Sansonetti, P. & Dehio, C. The secreted Ipa complex of Shigella flexneri promotes entry into mammalian cells. *Proceedings of the National Academy of Sciences* **93**, 1254-1258 (1996).
20. Reeves, A.Z. & Lesser, C.F. Transfer of Large Contiguous DNA Fragments onto a Low Copy Plasmid or into the Bacterial Chromosome. *Bio Protoc* **6** (2016).
21. Bahrani, F.K., Sansonetti, P.J. & Parsot, C. Secretion of Ipa proteins by Shigella flexneri: inducer molecules and kinetics of activation. *Infect Immun* **65**, 4005-4010 (1997).
22. Schmidt, F.I. et al. A single domain antibody fragment that recognizes the adaptor ASC defines the role of ASC domains in inflammasome assembly. *J Exp Med* **213**, 771-790 (2016).
23. Ingram, J.R. et al. PD-L1 is an activation-independent marker of brown adipocytes. *Nat Commun* **8**, 647 (2017).
24. Ingram, J.R. et al. Anti-CTLA-4 therapy requires an Fc domain for efficacy. *Proc Natl Acad Sci U S A* **115**, 3912-3917 (2018).
25. Ashour, J. et al. Intracellular expression of camelid single-domain antibodies specific for influenza virus nucleoprotein uncovers distinct features of its nuclear localization. *J Virol* **89**, 2792-2800 (2015).

26. Tremblay, J.M. et al. A single VHH-based toxin-neutralizing agent and an effector antibody protect mice against challenge with Shiga toxins 1 and 2. *Infect Immun* **81**, 4592-4603 (2013).
27. Qian, Z.G., Xia, X.X., Choi, J.H. & Lee, S.Y. Proteome-based identification of fusion partner for high-level extracellular production of recombinant proteins in Escherichia coli. *Biotechnol Bioeng* **101**, 587-601 (2008).
28. Zhang, G., Brokx, S. & Weiner, J.H. Extracellular accumulation of recombinant proteins fused to the carrier protein YebF in Escherichia coli. *Nature Biotechnology* **24**, 100-104 (2006).
29. Gao, D., Wang, S., Li, H., Yu, H. & Qi, Q. Identification of a heterologous cellulase and its N-terminus that can guide recombinant proteins out of Escherichia coli. *Microbial Cell Factories* **14**, 49 (2015).
30. Gao, D., Luan, Y., Liang, Q. & Qi, Q. Exploring the N-terminal role of a heterologous protein in secreting out of Escherichia coli. *Biotechnol Bioeng* **113**, 2561-2567 (2016).
31. Ulissi, U., Fabbretti, A., Sette, M., Giuliodori, A.M. & Spurio, R. Time-resolved assembly of a nucleoprotein complex between Shigella flexneri virF promoter and its transcriptional repressor H-NS. *Nucleic Acids Res* **42**, 13039-13050 (2014).
32. Morin, C.E. & Kaper, J.B. Use of stabilized luciferase-expressing plasmids to examine in vivo-induced promoters in the Vibrio cholerae vaccine strain CVD 103-HgR. *FEMS Immunol Med Microbiol* **57**, 69-79 (2009).
33. Ho, C.L. et al. Engineered commensal microbes for diet-mediated colorectal-cancer chemoprevention. *Nat Biomed Eng* **2**, 27-37 (2018).
34. Hwang, I.Y. et al. Engineered probiotic Escherichia coli can eliminate and prevent Pseudomonas aeruginosa gut infection in animal models. *Nat Commun* **8**, 15028 (2017).
35. Matsumoto, M. et al. Free D-amino acids produced by commensal bacteria in the colonic lumen. *Scientific Reports* **8**, 17915 (2018).
36. Mimee, M. et al. An ingestible bacterial-electronic system to monitor gastrointestinal health. *Science* **360**, 915-918 (2018).
37. Graham, D.B. & Xavier, R.J. Pathway paradigms revealed from the genetics of inflammatory bowel disease. *Nature* **578**, 527-539 (2020).
38. Neurath, M.F. Current and emerging therapeutic targets for IBD. *Nature Reviews Gastroenterology & Hepatology* **14**, 269-278 (2017).
39. Sandborn, W.J. & Loftus, E.V. Balancing the risks and benefits of infliximab in the treatment of inflammatory bowel disease. *Gut* **53**, 780-782 (2004).
40. Wirtz, S. et al. Chemically induced mouse models of acute and chronic intestinal inflammation. *Nat Protoc* **12**, 1295-1309 (2017).
41. Neurath, M.F. et al. Predominant pathogenic role of tumor necrosis factor in experimental colitis in mice. *Eur J Immunol* **27**, 1743-1750 (1997).
42. Steidler, L. et al. Treatment of murine colitis by Lactococcus lactis secreting interleukin-10. *Science* **289**, 1352-1355 (2000).
43. Vandenbroucke, K. et al. Orally administered L. lactis secreting an anti-TNF Nanobody demonstrate efficacy in chronic colitis. *Mucosal immunology* **3**, 49-56 (2010).
44. Kimoto, H., Nomura, M., Kobayashi, M., Mizumachi, K. & Okamoto, T. Survival of lactococci during passage through mouse digestive tract. *Can J Microbiol* **49**, 707-711 (2003).
45. Zhang, C. et al. Ecological robustness of the gut microbiota in response to ingestion of transient food-borne microbes. *The ISME Journal* **10**, 2235-2245 (2016).
46. Drouault, S., Corthier, G., Ehrlich, S.D. & Renault, P. Survival, physiology, and lysis of Lactococcus lactis in the digestive tract. *Appl Environ Microbiol* **65**, 4881-4886 (1999).

47. McKay, R. et al. A platform of genetically engineered bacteria as vehicles for localized delivery of therapeutics: Toward applications for Crohn's disease. *Bioeng Transl Med* **3**, 209-221 (2018).
48. Riglar, D.T. et al. Engineered bacteria can function in the mammalian gut long-term as live diagnostics of inflammation. *Nature Biotechnology* **35**, 653-658 (2017).
49. Aurand, T.C. & March, J.C. Development of a synthetic receptor protein for sensing inflammatory mediators interferon-γ and tumor necrosis factor-α. *Biotechnol Bioeng* **113**, 492-500 (2016).
50. McMahon, C. et al. Yeast surface display platform for rapid discovery of conformationally selective nanobodies. *Nature structural & molecular biology* **25**, 289-296 (2018).
51. Zimmermann, I. et al. Synthetic single domain antibodies for the conformational trapping of membrane proteins. *Elife* **7** (2018).
52. Widmaier, D.M. et al. Engineering the Salmonella type III secretion system to export spider silk monomers. *Mol Syst Biol* **5**, 309 (2009).
53. Stritzker, J. et al. Tumor-specific colonization, tissue distribution, and gene induction by probiotic Escherichia coli Nissle 1917 in live mice. *Int J Med Microbiol* **297**, 151-162 (2007).
54. Nougayrède, J.-P. et al. A Toxic Friend: Genotoxic and Mutagenic Activity of the Probiotic Strain Escherichia coli Nissle 1917. *mSphere* **6**, e00624-00621 (2021).
55. Arthur, J.C. et al. Intestinal inflammation targets cancer-inducing activity of the microbiota. *Science* **338**, 120-123 (2012).
56. Pleguezuelos-Manzano, C. et al. Mutational signature in colorectal cancer caused by genotoxic pks(+) E. coli. *Nature* **580**, 269-273 (2020).
57. Olier, M. et al. Genotoxicity of Escherichia coli Nissle 1917 strain cannot be dissociated from its probiotic activity. *Gut Microbes* **3**, 501-509 (2012).
58. Massip, C. et al. Deciphering the interplay between the genotoxic and probiotic activities of Escherichia coli Nissle 1917. *PLOS Pathogens* **15**, e1008029 (2019).
59. Wallenstein, A. et al. ClbR Is the Key Transcriptional Activator of Colibactin Gene Expression in Escherichia coli. *mSphere* **5**, e00591-00520 (2020).

Figure Legends

Figure 1. Schematic overview. (a) Schematic design of the PROT$_3$EcT (PRObiotic Type 3 secretion *E. coli* Therapeutic) platform, in which the bacteria chassis is engineered with a modified type III secretion apparatus (T3SA) and a therapeutic payload. (b) Schematic of PROT$_3$EcT delivering its therapeutic payload directly to the gut lumen.

Figure 2. *E. coli* engineered with a modified T3SA efficiently secrete proteins into their surroundings. Secretion of FLAG-tagged OspC2 by the indicated strains was monitored by liquid secretion assays sampling at 30-minutes (a, b, e), 6 hours (c) or over a time course at the indicated times (f). (a, b, e, f) Immunoblots of FLAG-tagged OspC2 and GroEL. (c) Coomassie blue stained gel. For each liquid secretion assay, except for (f), the supernatants and pellets were normalized to the lowest OD_{600}. In (f), samples were loaded without normalizing for the OD_{600}. In each western blot panel, the images shown are from the same exposure of membranes immunoblotted with designated antibodies. (d) Schematic of PROT$_3$EcT-1 transformed with pNG-virB and pDSW206-OspC2-FLAG plasmids treated with IPTG. (g) The ability of strains to invade intestinal epithelial cells (HCT8) was determined by gentamicin protection assays. Each data point represents a single bacterial culture. Means are marked with horizontal lines. Data were analyzed using one-way ANOVA with Tukey's post-hoc test; for all strain comparisons to *Shigella* *** $P < 0.0001$; ns = not significant (both $P > 0.999$). Data in each panel is representative of results from at least 2 independent experiments. CR = Congo red. P = whole cell pellet lysates, S = supernatant fractions.

Figure 3. PROT$_3$EcT can be engineered to secrete nanobodies. 6 h liquid secretion assays monitoring the secretion of (a) HA-tagged Nb^{ASC} with different N-terminal type III secretion signals, (b) HA-tagged-Nb^{ASC}, -Nb$^{PD\text{-}L1}$, -Nb$^{CTLA\text{-}4}$ and -Nb^{NP1} with an N-terminal OspC2 secretion

signal (OspC2ss), (c) FLAG-tagged Nb^{Stx2} monomer (1x), dimer (2x) and trimer (3x) with N-terminal OspC2ss and (d) FLAG-tagged Nb^{Stx2} dimer modified with an N-terminal OspC2ss (OspC2ss-Nb^{2x}). Data in each panel is representative of results from at least 2 independent experiments. P = whole cell pellet lysates, S = supernatant fractions

Figure 4. Development of nanobody-secreting constitutively active $PROT_3EcT$. 2xNb^{Stx2} secretion was monitored for 18 h to compare (a) the performance of different *virB* promoters in $PROT_3EcT$-1, (c) plasmid encoded (PL) versus chromosomally integrated (INT) *virB* under the control of P_{J23119} in $PROT_3EcT$-1 and (d) P*tac* (P_{IPTG}) versus P_{J23108} driven 2xNb^{Stx2} expression/secretion in $PROT_3EcT$-3. (b) Schematic of PROT3EcT-3 with virB under a constitutive promoter (Pc) integrated and pDSW206-OspC2-2xNb^{Stx2}. (e) Schematic of $PROT_3EcT$-4 with pCPG-*alr*-P*J23108*-OspC2-2xNb^{Stx2}. (f) 2xNb^{Stx2} expression and secretion in $PROT_3EcT$-3 and $PROT_3EcT$-4 grown in the presence or absence of ampicillin (Amp); secretion was monitored for 18 h. (g) Growth rate of strains in LB media without antibiotics. Data are presented as the mean ± SD and are representative of results from at least 2 independent experiments. Data were analyzed using two-way ANOVA with Tukey's post-hoc test. ns = not significant compared to EcN ($PROT_3EcT3$, P=0.7622; $PROT_3EcT4$ + pCGP-*alr*, P=0.9612; $PROT_3EcT$-4 + pCGP-*alr*-P*J23108*-OspC2-2xNb^{Stx2}, P=0.5957)

Figure 5. **$PROT_3EcT$ stably colonizes the gastrointestinal tract of mice.** (a) Study design. C57/BL6 mice were orally gavaged with 10^8 CFU of EcN or $PROT_3EcT$-4 and fecal pellets were sampled at the times indicated. (b) Shed bacterial titers as measured by plating homogenates of fecal pellets on selective media and enumerating colonies. Data are presented as the mean ± SEM, n=4 mice per group and represent at least 2 independent experiments. Data were

552 analyzed using two-way ANOVA with Tukey's post hoc test. ns = not significant (P=0.4846). (c)
553 6 h plate secretion assay of colonies of PROT3EcT-4 shed from mice at 14 dpi. Membranes are
554 removed and probed with an anti-FLAG to monitor Nb^{TNF} secretion. (d-e) Bioluminescent
555 imaging of intestinal explants from individual mice inoculated with strains expressing a
556 constitutive bioluminescent reporter pMM543 (d) or pMxiE-lux+ +pNG162-lpgC (e) at 8 dpi. Dpi
557 = days post inoculation.

558

559 **Figure 6**. **TNF-$PROT_3$EcT inhibits the development of disease in a mouse model of colitis.**
560 (a) 6 h liquid secretion assays monitoring the secretion of FLAG-tagged Nb^{TNF} monomer (1x)
561 and homodimer (2x) fused to the N-terminal OspC2ss by $PROT_3$EcT-1. P = whole cell lysate, S
562 = precipitated supernatant. (b) Viability of L929 cells following incubation with 0.2 ng/ml of
563 murine TNFα plus supernatants from PROT3EcT-1 induced to secrete the Nb^{TNF} dimer,
564 $PROT_3$EcT-1 with empty vector and purified Nb^{TNF} dimer. Sup = supernatant. Data were
565 analyzed using a two-way ANOVA with Tukey's post hoc test ns = not significant (P=0.9980) (c)
566 Study design. BALB/c mice received TNBS (2 mg, enema in 50% ethanol) plus oral gavages of
567 PBS (n=10) or an inoculum of 10^8 CFU of $PROT_3$EcT-4 (n=10) or TNF-$PROT_3$EcT-4 (n=9) at
568 the times indicated and were sacrificed at 5 days post TNBS. (d) Shed bacteria. P=0.3230. (e)
569 Body weight change (%). *denotes comparison to PBS group, P=0.0118; # denotes comparison
570 to $PROT_3$EcT-4; day 1, P=0.0238; day 2, P=0.0122. (f) Colon length. *, P=0.0219; ***,
571 P=0.0004. (g) Histologic colitis scores. top *, P=0.0231; bottom *, P=0.0141. (h) Representative
572 histology of colon sections stained with hematoxylin and eosin from each experimental group. (i)
573 Study design. Mice were treated with TNBS plus oral gavages of PBS (n=10) or an inoculum of
574 10^8 CFU of $PROT_3$EcT-4 (n=9) or TNF-$PROT_3$EcT-4 (n=10) and sacrificed at 2 days post TNBS.
575 An additional group of mice treated with ethanol alone was included (n=5). (j) Shed bacteria.
576 P=0.1758. (k) Body weight change (%). *denotes comparison to PBS, day 1, P=0.0002, day 2,

P<0.0001; #denotes comparison to PROT$_3$EcT-4, day 1, P=0.054, day 2, P<0.0001. (l) Colon length. *, P=0.0184; **, P=0.0029. (m) Histologic colitis scores. **, P=0.0045. Colon homogenates were analyzed for the levels of TNFα (n) (***, P=0.0005, *, P=0.0433), IL-6 (o) (right *, P=0.0356; left *, P=0.0322) and IL-10 (p) by ELISA. (d-g, j-p) Data were combined from 2 independent experiments and are presented as individual values ± SEM (f-g, l-p) or mean ± SEM (d-e, j-k). Data were analyzed using a Kruskal-Wallis test with Dunn's multiple correction test (f, g, l-p) or a two-way ANOVA with Tukey's post hoc test (j, k). TNBS = 2,4,6-Trinitrobenzenesulfonic acid. EtOH = ethanol.

Acknowledgements

The authors thank Pam Silver for critically reading the manuscript. Drs. Gökhan S. Hotamışlıgil and Karen Inouye at the Harvard T. H. Chan School of Public Health for their assistance with the IVIS experiments and Sue Chapman for assistance in the L929/TNF assay. Some graphics were created with BioRender.com. Supported by NIH grants (AI064285, DK113599), a Kenneth Rainin Foundation grant and the Brit d'Arbeloff Research Scholar award to C.F.L, Massachusetts General Hospital Executive Committee on Research Fund for Medical Discovery Postdoctoral Fellowship Awards to C.G.P and A.Z.R., and an Endeavour Australia Research Fellowship and a Crohn's & Colitis Foundation Research Fellow Award, award number 654758, to J.P.L. The authors thank members of the Lesser, Garrett, Leong and Goldberg labs for helpful discussions and suggestions.

Author Contributions

J.P.L., C.G.P., A.Z.R., J.M.L., C.B.S., W.S.G., and C.F.L designed experiments, interpreted data. J.P.L., C.G.P., A.Z.R., N.S., J.M.T and U.P. performed experiments and analyzed data.

F.I.S and H.L.P generated and provided plasmids. J.N.G performed the histology scoring. J.P.L and C.F.L wrote the manuscript. C.G.P., A.Z.R., F.I.S, J.M.L., C.B.S., and W.S.G., edited the manuscript.

Competing Interests statement

The authors declare no competing financial interests. Related to this work, C.F.L is on the scientific advisory board (SAB) of Synlogic Therapeutics and W.S.G is on the SABs of Kintai Therapeutics, SanaRx, Evelo Biosciences and Tenza. F.I.S. is a consultant and shareholder of IFM Therapeutics and NewCo (to be changed if public), as well as cofounders and shareholders of Dioscure Therapeutics SE.

Figure 1

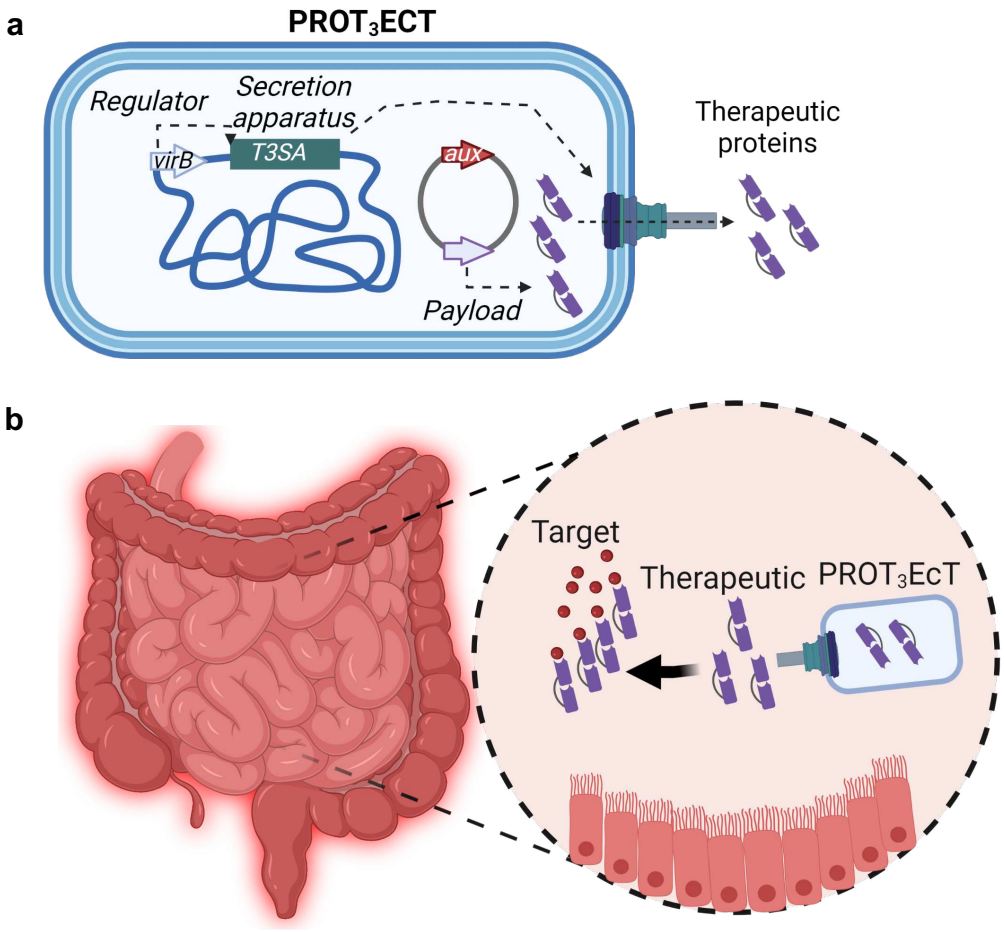
a
PROT3ECT
Regulator
Secretion apparatus
virB
T3SA
aux
Payload
Therapeutic proteins
b
Target
Therapeutic
PROT3ECT

Figure 2

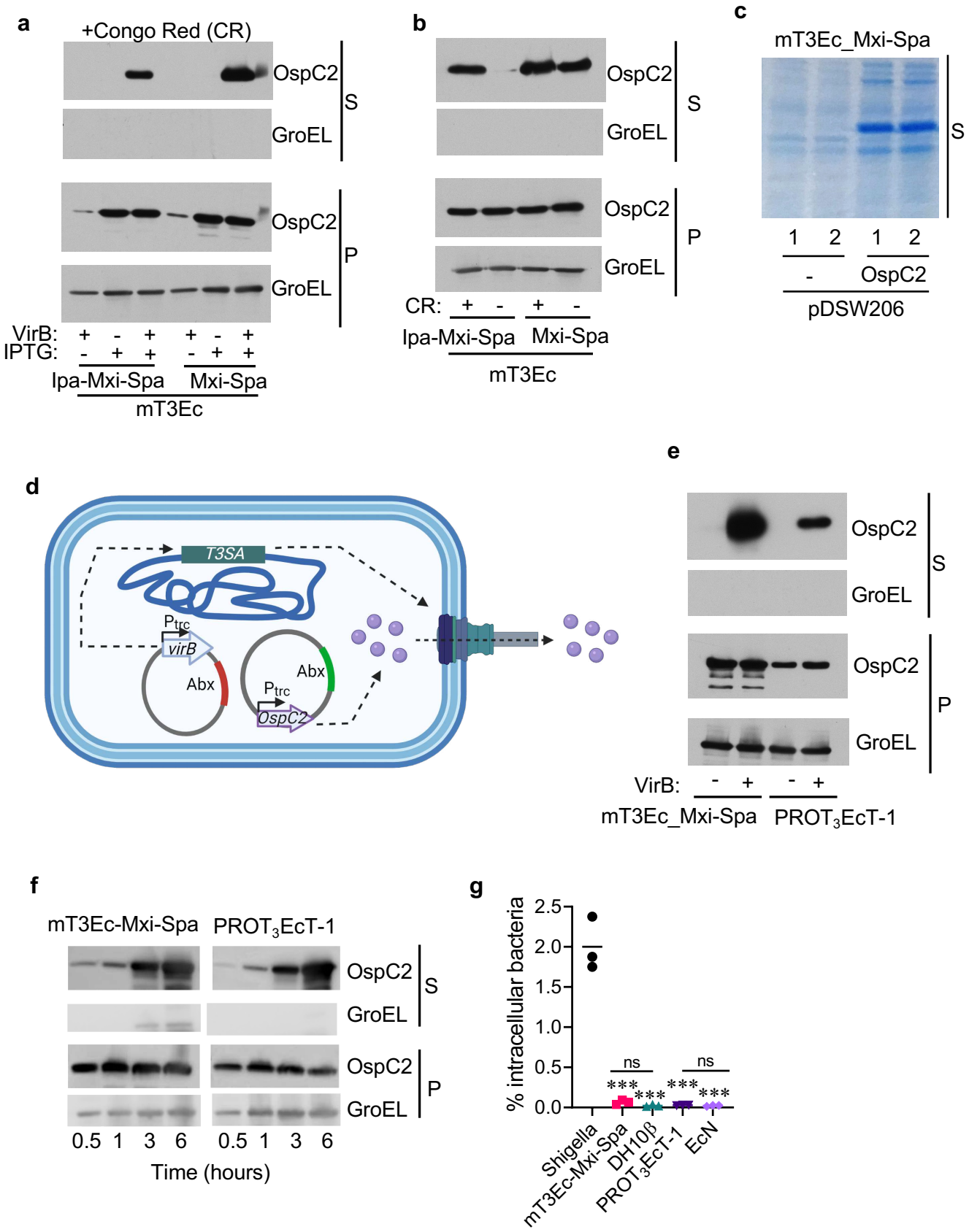
a
+Congo Red (CR)
OspC2
GroEL
S
P
VirB:
IPTG:
Ipa-Mxi-Spa
Mxi-Spa
mT3Ec
b
CR:
Ipa-Mxi-Spa
Mxi-Spa
mT3Ec
c
mT3Ec_Mxi-Spa
1 2 1 2
-
OspC2
pDSW206
d
T3SA
Ptrc
virB
Abx
OspC2
e
VirB:
mT3Ec_Mxi-Spa
PROT3EcT-1
f
mT3Ec-Mxi-Spa
PROT3EcT-1
0.5 1 3 6 0.5 1 3 6
Time (hours)
g
% intracellular bacteria
2.5
2.0
1.5
1.0
0.5
0.0
ns
***
Shigella
mT3Ec-Mxi-Spa
DH10β
PROT3EcT-1
EcN

Figure 3

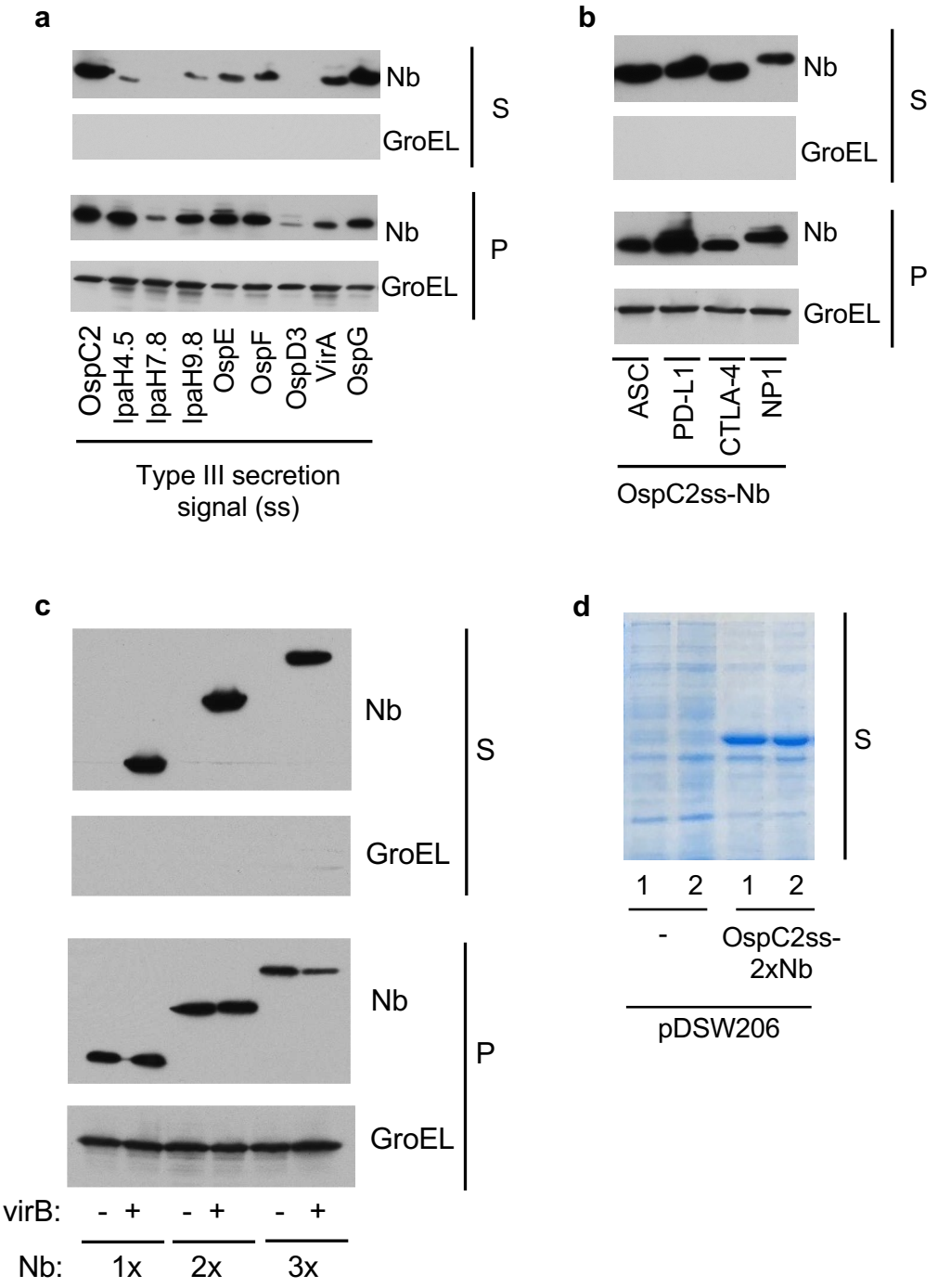
a
Nb
GroEL
S
Nb
GroEL
P
OspC2
IpaH4.5
IpaH7.8
IpaH9.8
OspE
OspF
OspD3
VirA
OspG
Type III secretion signal (ss)
b
Nb
GroEL
S
Nb
GroEL
P
ASC
PD-L1
CTLA-4
NP1
OspC2ss-Nb
c
Nb
GroEL
S
Nb
GroEL
P
virB: - + - + - +
Nb: 1x 2x 3x
d
S
1 2 1 2
-
OspC2ss-2xNb
pDSW206

Figure 4

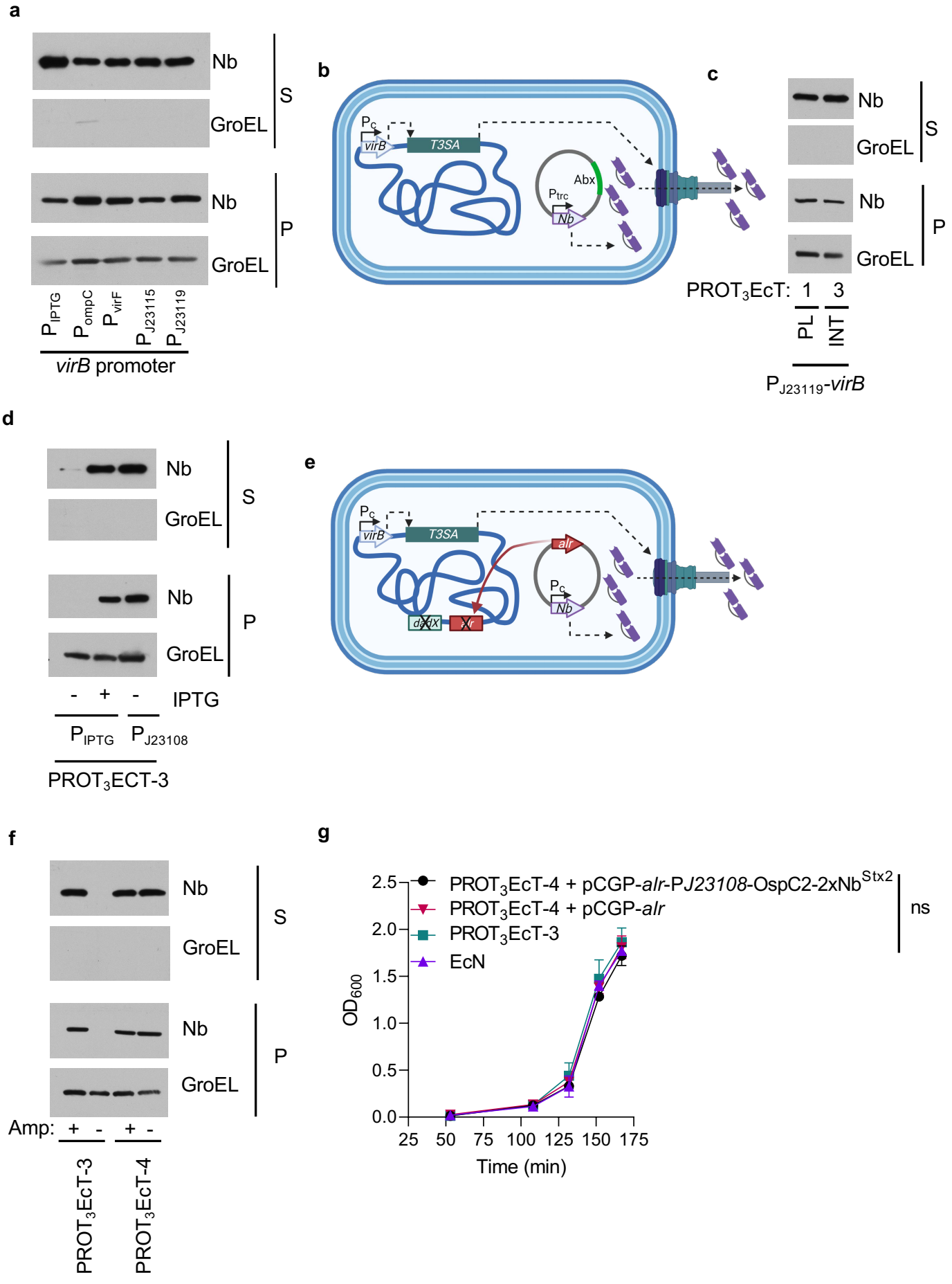
a
Nb
GroEL
S
P
P_{IPTG}
P_{ompC}
P_{virF}
P_{J23115}
P_{J23119}
virB promoter
b
P_c
virB
T3SA
Abx
P_{trc}
Nb
c
PROT$_3$EcT: 1 3
PL
INT
P_{J23119}-*virB*
d
P_{IPTG}
P_{J23108}
PROT$_3$ECT-3
IPTG
e
alr
dadX
Xr
f
Amp:
PROT$_3$EcT-3
PROT$_3$EcT-4
g
PROT$_3$EcT-4 + pCGP-*alr*-P*J23108*-OspC2-2xNb^{Stx2}
PROT$_3$EcT-4 + pCGP-*alr*
PROT$_3$EcT-3
EcN
ns
OD_{600}
Time (min)

Figure 5

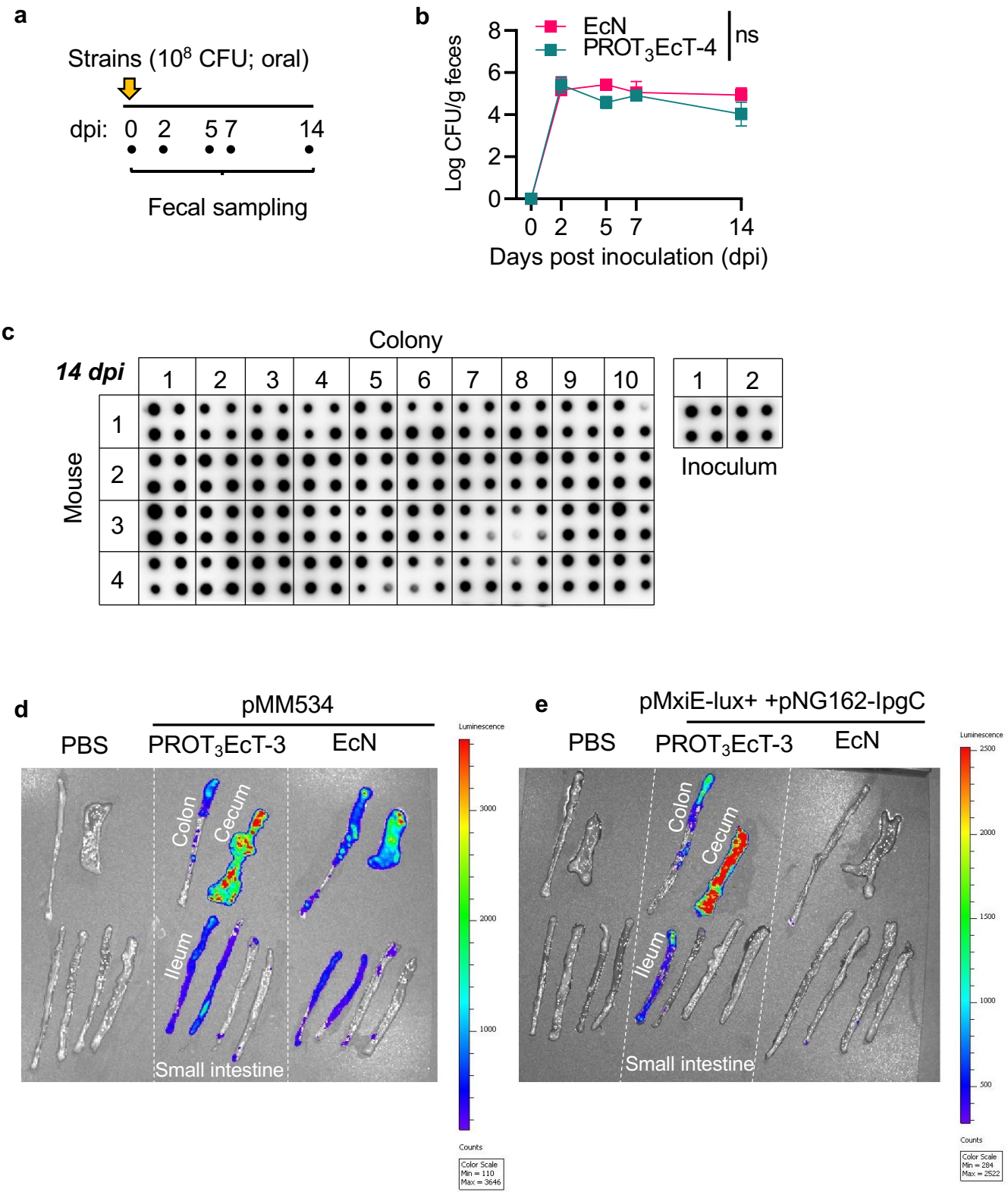
a
Strains (10^8 CFU; oral)
dpi: 0 2 5 7 14
Fecal sampling
b
EcN
PROT3EcT-4
ns
Log CFU/g feces
Days post inoculation (dpi)
c
Colony
14 dpi
Mouse
Inoculum
d
pMM534
PBS
PROT3EcT-3
EcN
Colon
Cecum
Ileum
Small intestine
Luminescence
Counts
e
pMxiE-lux+ +pNG162-IpgC
PBS
PROT3EcT-3
EcN
Colon
Cecum
Ileum
Small intestine
Luminescence
Counts

Figure 6

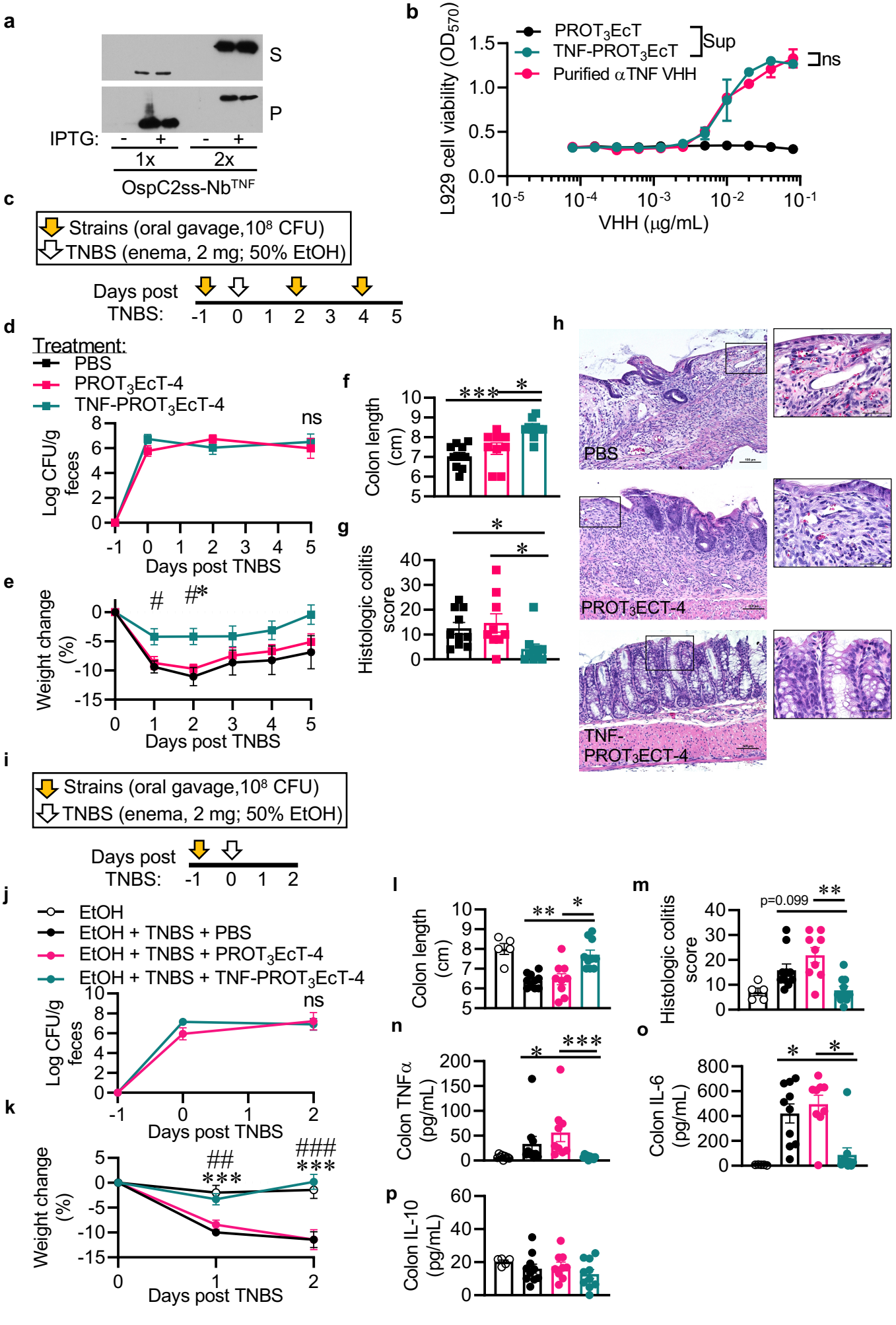
a
S
P
IPTG: - + - +
1x 2x
OspC2ss-Nb^TNF
b
PROT3EcT
TNF-PROT3EcT
Purified αTNF VHH
Sup
ns
L929 cell viability (OD570)
VHH (μg/mL)
c
Strains (oral gavage,10^8 CFU)
TNBS (enema, 2 mg; 50% EtOH)
Days post TNBS: -1 0 1 2 3 4 5
d
Treatment:
PBS
PROT3EcT-4
TNF-PROT3EcT-4
Log CFU/g feces
Days post TNBS
e
Weight change (%)
Days post TNBS
f
Colon length (cm)
g
Histologic colitis score
h
PBS
PROT3ECT-4
TNF-PROT3ECT-4
i
Strains (oral gavage,10^8 CFU)
TNBS (enema, 2 mg; 50% EtOH)
Days post TNBS: -1 0 1 2
j
EtOH
EtOH + TNBS + PBS
EtOH + TNBS + PROT3EcT-4
EtOH + TNBS + TNF-PROT3EcT-4
Log CFU/g feces
Days post TNBS
k
Weight change (%)
Days post TNBS
l
Colon length (cm)
m
Histologic colitis score
p=0.099
n
Colon TNFα (pg/mL)
o
Colon IL-6 (pg/mL)
p
Colon IL-10 (pg/mL)

Methods

Plasmids, bacterial strains, cell lines and mouse strains.

Plasmids and strains are summarized in Supplementary Tables 2 and 3, respectively. Sequences of oligos and DNA inserts are summarized in Supplementary Tables 4 and 5, respectively. All gateway entry clone inserts were sequence verified. Synthetic DNA fragments were purchased from Integrated DNA technologists (IDT) or Genewiz. All restriction enzymes purchased from New England Biolabs. L929 fibroblast cells and HCT8 cells were grown as recommended by the American Type Culture Collection (ATCC). C57BL/6J mice were used for colonization studies and BALB/cJ mice for the TNBS colitis models. All mice were obtained from The Jackson Laboratory and were housed in microisolator cages in the barrier facility of Harvard T.H. Chan School of Public Health. Animal experiments were approved and carried out in accordance with Harvard Medical School's Standing Committee on Animals and the National Institutes of Health guidelines for animal use and care.

Plasmid construction

$Nb^{PD\text{-}L1}$, $Nb^{CTLA\text{-}4}$, Nb^{ASC} and Nb^{NP1} Gateway compatible destination vectors: Gateway compatible destination vectors that enable the in-frame introduction of sequences upstream of $Nb^{PD\text{-}L1}$, $Nb^{CTLA\text{-}4}$, Nb^{ASC} and Nb^{NP1} were generated by using Gibson cloning (NEB) to join (1) PCR amplified Nb-HA fragments from pHEN6 VHH52 [anti-IAV NP]/VHH KV 022[anti-IAV NP]/VHH PD-L1 B3/VHH CTLA-4 H11/VHH ASC with oligomers (P1/P2) and (2) pDSW206-ccdB-MyoD NS with oligomers (P3/P4). Each VHH containing fragment was introduced into the pDSW206 based vectors via Gibson cloning (NEB). Resulting clones were sequence verified. The resulting plasmids are referred to as pDSW206-ccdB-Nb* (* = name of Nb present in construct).

$Nb^{PD\text{-}L1}$, $Nb^{CTLA\text{-}4}$, Nb^{ASC} and Nb^{NP1} expression plasmids. A variety of type III secretion signal sequences were introduced into pDSW206-ccdB-Nb^{ASC} via LR reaction using pENTR-secretion sequence entry clones. An OspC2 secretion signal (OspC2ss) was introduced into pDSW206-ccdB-$Nb^{PD\text{-}L1}$, pDSW206-ccdB-Nb^{CTLA4} or pDSW206-ccdB-Nb^{NP1} via a LR reaction with pENTR-OspC2ss.

Alr plasmids. A DNA fragment containing *alr* and its native promoter with flanking attB1 and attB2 sites PCR-amplified from EcN using oligomers (P5/P6) was introduced into pDONR221 via a BP reaction followed by pCMD136-*ccdB*-FLAG via an LR reaction. The resulting plasmid, pCMD136-*alr*, was used as a template for nested PCR with oligomers (P7/P8, P7/P9 and P10/P11) to generate a DNA fragment (*BspHI*-P*alr-alr-T7t-AseI*) that was introduced via traditional cloning into pDSW206[1] digested with *NcoI*/*NdeI* to create pCGP-*alr*.

Nb^{STX2} expression plasmids. A synthetic DNA fragment [attB1-OspC2ss-three Nb^{Stx2} (JFG-H6, JFD-A5 and JGH-G1)-E-tag-attB2] was introduced into pDONR221 via a BP reaction followed by pDSW206-ccdB-3xFLAG via an LR reaction to create pDSW206-OspC2ss-3xNb^{Stx2}**.** Dimeric (JFG-H6, JFD-A5) and monomeric (JFG-H6) DNA fragments PCR amplified from pDSW206-OspC2ss-3xNb^{Stx2} using oligomers (P12/P13 and P12/P14) were introduced into pDONR221 via a BP reaction followed by pDSW206-*ccdB*-3xFLAG via LR reactions to create pDSW206-OspC2ss-2xNb^{Stx2} and pDSW206-OspC2ss-Nb^{Stx2}.

To replace the IPTG-inducible P*trc* promoter and the lacIq repressor in pDSW206-OspC2ss-2xNb^{Stx2} with a constitutive promoter, two complementary oligos (P15/P16) were annealed to create a BBa_J23115 promoter (Anderson Collection) with cohesive *SphI* and *SacI* ends. The dsDNA fragment was cloned into *SphI/SacI* digested pDSW206-OspC2ss-2xNb^{Stx2} to create pDSW206-J23115-OspC2ss-2xNb^{Stx2}. The (PJ23115-OspC2ss-2xNb^{Stx2}) fragment in this plasmid was PCR amplified (P17/P18) and introduced into *KpnI/XbaI*-digested pCGP-*alr* to

create pCGP-*alr*-PJ23115-OspC2ss-2xNb^{Stx2}. Two complementary oligos (P19/P20) were annealed to create a BBa_J23018 (Anderson Collection) promoter with cohesive *SacI* ends. The dsDNA fragment was cloned into *SacI*-digested pCGP-*alr*-PJ23115-OspC2ss-2xNb^{Stx2} replacing PJ23115 to create pCGP-*alr*-PJ23108-OspC2ss-2xNb^{Stx2}.

OsmY-, N20-Cel-CD-, Cel-CD- and YebF- Nb^{Stx2} expression plasmids. Synthetic DNA fragments composed of the following *E. coli* codon optimized components [attB1-RBS-(OsmY or N20-Cel-CD or Cel-CD or Yeb)-FL-2xNb^{Stx2}-attB2] were introduced into pDONR221 via BP reactions followed by pDSW206-ccdB-3xFLAG[2] via LR reactions to create pDSW206-OsmY-Nb^{Stx2}, pDSW206-N20-CelCD-Nb^{Stx2}, pDSW206-CelCD-Nb^{Stx2} and pDSW206-YebF-Nb^{Stx2}.

Nb^{TNF} expression plasmids. A synthetic DNA fragment [attB1--OspC2ss-Nb^{TNF}-attB2] was introduced into pDONR221 via a BP reaction followed by pDSW206-*ccdB*-FLAG via an LR reaction to create pDSW206-OspC2ss-Nb^{TNF}. A DNA fragment composed of homodimer Nb^{TNF} fused to an OspC2ss was generated using SOEing PCR with oligomers (P12/P22 and P21/P18) to generate attB1-OspC2ss-2xNb^{TNF}-attB2. The resulting fragment was introduced in pDONR221 followed by pDSW206-*ccdB*-FLAG via BP and LR reaction to generate pDSW206-OspC2-2xNb^{TNF}. pDSW206-PJ23115-OspC2ss-2xNb^{TNF} and pDSW206-alr-PJ23115-OspC2ss-2xNb^{TNF} were constructed as previously described for Nb^{Stx2}.

VirB expression plasmids. Entry clones that contain *virB* under the control of various promoters were obtained via SOEing PCR using two synthetic DNA fragments and oligomers (P23/P24). One synthetic DNA fragment contained a promoter flanked by an upstream attB site and downstream by 40 bp of homology to *virB*[1]. The second DNA fragment contained the open reading frame of *virB* codon-optimized for expression in *E. coli* with an upstream RBS and a downstream stop codon followed by an attB site. The RBS Calculator tool version 1.1[1], with organism option as *E. coli* str. K-12 substr. MG1655, was used to choose the RBS. The

resulting DNA fragments were introduced into pDONR221 via a BP reaction followed by pCMD136-*ccdB*-FLAG via an LR reaction. pTKIP-PJ23119-*virB* was generated by PCR amplifying P*J23119-virB* from pCGP-PJ23119-*virB*-Nb with oligomers (P25/P26) that add a 5´ *KpnI* site and a 3´ rrnB-homology region. Using pCMD136 as a template, the rrnB terminator was amplified with a 5´ *virB*-homology region and a 3´ *HindIII* site using oligomers (P27/P28). The two fragments were fused together by SOEing PCR using oligomers (P25/P28). The product was digested with *KpnI* and *HindIII* and ligated into the polylinker of pTKIP-*hph.*

MxiE-Luciferase expression plasmid. A DNA fragment that contains a MxiE-promoter was PCR amplified from pTSAR1Ud2.4s[2] using oligomers (P29/P30) that add flanking 5´ *XhoI* and 3´ *KpnI* restriction sites and an RBS. The digested PCR product was ligated into *XhoI/KpnI* pMM534 to generate pMxiE-lux.

Strain construction

PROT$_3$ECT-1 and PROT$_3$ECT-2. A synthetic 1.3 kb landing pad insertion site was introduced into the *atg/gid* loci of EcN and *E. coli* HS to generate EcN-LP$^{atp/gid}$ and EcHS- LP$^{atp/gid}$ using the lambda red recombination system and the pTKRED helper plasmid[3]. The landing pad fragment was PCR amplified from pTKIP-*tetA* with oligos (P31/P32) to introduce homology to the *atg/gid* locus and integration was confirmed by PCR with oligo pairs (P33/P34 and P35/P36).The pmT3SA plasmid which contains the 20 kb Mxi-Spa operons flanked by LP and *SceI* sequences was introduced into EcN-LP$^{atp/gid}$ and EcHS-LP$^{atp/gid}$ via triparental mating: donor (DH10ß/pT3SA), helper HB101 (pRK2073[4]) and recipient (EcN- or EcHS-LP$^{atp/gid}$/pKD46). pKD46-cured EcN- and HS-LP$^{atp/gid}$ containing pT3SA were transformed with pTKRED and landing pad recombination system was used to generate PROT$_3$ECT-1 and PROT$_3$ECT-2. KAN resistant/TET susceptible transformants were screened for proper integration junctions by PCR with oligo pairs (P33/P37 and P35/P38).

PROT$_3$ECT-3. PROT$_3$ECT-1 was modified with a landing pad at its *yieN/trkB* locus to create PROT$_3$ECT-1-LP$^{yie/trk}$. By PCR, the landing pad with appropriate homology regions was amplified with oligos (P39/P40) and its integration was confirmed with P41/P34 and P42/P36. PROT$_3$ECT-1-LP$^{yie/trk}$ was transformed with pTKred and pTKIP-PJ23119-*virB* and the landing pad platform was used to introduce the VirB expression construct into the chromosome. Integration was confirmed by PCR with oligos P43/P28 and P44/P27.

PROT$_3$ECT-4. After first resolving the KAN^R marker previously used to introduce the Mxi-Spa operons into PROT$_3$ECT-1 using the FLP recombinase, the lambda red recombination system was used to sequentially delete *alr* and *dadX* from PROT$_3$ECT-3 using oligomers (P45/P46 and P47/P48)[5]. The KAN^R was removed from the *alr* locus, before proceeding to delete *dadX*. Deletions were confirmed by PCR with oligomers (P49/P50 and P51/P52, respectively).

Gentamicin protection assay.

HCT8 cells were seeded in 96-well plates (4×10^4 cells per well) for 18 h prior to exposure to bacteria. Bacteria grown overnight with aeration at 37°C were back-diluted and subcultured for one hour before the addition of IPTG (1 mM). One hour later, the HCT8 cells were infected at an MOI of 100. After 30 min, gentamicin (50 µg/mL) was added, and 30 minutes later, cells were lysed with 1% triton X-100 in PBS. Bacteria were plated and enumerated. Percentage of internalized bacteria was determined by calculating the ratio of gentamicin resistant bacteria to the initial inoculum.

Liquid secretion assays.

Liquid Secretion assays were performed as previously described[36] with some modifications. Overnight cultures of *E. coli* grown in LB (Luria broth) were back diluted 1:50. Once cultures reached OD_{600} of 1.2-1.5, the bacteria were pelleted and resuspended in fresh media or PBS

and incubated for the times indicated. IPTG (1 mM, Sigma) was added when studying P*trc* regulated *virB* and/or *nb*. When indicated, bacteria were exposed to 10 µM Congo red (Sigma). After designated periods of time, total cell and supernatant fractions were separated by centrifugation at 20,000g for 2 min. The cell pellet was taken as the total cell fraction. The supernatant fraction was subjected to a second centrifugation step. To account for differences in bacterial titers, the volume of protein loading dye (40% glycerol, 240 mM Tris/HCl pH 6.8, 12% SDS, 0.04% bromophenol blue, 5% beta-mercaptoethanol) used to resuspend each sample was normalized by the OD_{600} reading of the slowest growing culture. For some assays, as indicated in the text, samples were not normalized. The pellet was resuspended in 100 µL or more protein loading dye, depending on the OD_{600}, and 5 µL was loaded onto a 10% SDS-PAGE gel for analysis. Proteins in the supernatant were precipitated with trichloroacetic acid (TCA) (10% v/v) and resuspended in 50 µL or more protein loading dye, depending on the OD_{600}. Ten microliters of TCA-precipitated supernatant samples were loaded onto a 12% SDS-PAGE gel for analysis. Proteins were transferred to nitrocellulose membranes and immunoblotted with mouse anti-FLAG (1:10,000, clone M2, Sigma,), mouse anti-HA (1:1000, clone 16B12, Biolegend) or rabbit anti-GroEL (1:100,000, G6532, Sigma). Alternatively, SDS-PAGE gels were stained with GelCode™ Blue Stain Reagent (Thermo Fisher Scientific), per the manufacturer's instructions.

Solid plate secretion assay.

Solid plate secretion assays were performed as previously described. Briefly, single colonies grown overnight in 96 well plates were quad spotted onto a solid agar plate[7]. After overnight growth, a robotic 384-pin tool is used to transfer equivalent amounts of bacteria to a second media containing plate over which a nitrocellulose membrane was immediately laid. After 6 hrs at 37°C, the membrane was removed, washed, and immunoblotted for protein of interest.

Fecal shedding assay.

Fecal pellets were collected and weighed. A 10x volume of PBS was added and the samples homogenized by pipetting and mashing using wide mouth pipette tips before being serially diluted and plated on MacConkey agar plates with antibiotics. After overnight incubation at 37 ^{o}C colonies were counted and the total number of CFU estimated.

In vitro luciferase monitoring.

In a 96 well white plate, 1:100 dilutions of overnight bacterial cultures were incubated at 37ºC with shaking for 5 h. Readings were performed on a SpectraMax i3x Multi-Mode Microplate Detection Platform (Molecular devices).

In vivo luminescence assays.

To image luciferase-expressing bacteria in the GI tract, mice pre-treated for 1 day with kanamycin (1 g/L) and spectinomycin (2 g/L) in their drinking water were orally gavaged with 10^8 CFU of PROT3EcT-3 or EcN harboring the constitutive luciferase or MxiE reporter plasmids. After sacrificing the mice, the cecum, colon and small intestine were harvested, the contents gently removed, and the tissues placed on a black mat for imaging using an IVIS Spectrum CT. Tissues were imaged using a luminescence filter, with field of view (FOV) = *D* (22.2 cm), fstop = 1 and large binning. Data was analyzed using Living Image Software 4.3.1.

Discovery and characterization of Nbs targeting murine TNFα.

Two alpacas were each immunized once with 200 µg murine (m)TNF-α (Biolegend 575204) in CpG/alum adjuvant, followed by four boosters with 100 µg mTNFα in alum adjuvant only. Nb display phage library construction, panning and screening were done as previously described[8]. Given that the number of unique Nb families obtained in first panning was low, it was repeated with mTNFα bound to JTT-B10 Nb, a Nb obtained in the initial screen. This second panning yielded 20 unique mTNFα-binding Nb families. The coding sequences of representative

members of each anti-TNF-a family were introduced into (Novagen) and expressed as thioredoxin, 6-His, E-tag fusion proteins in *E. coli* Rosetta-gami 2 (DE3) pLacI (Novagen) as fusions to thioredoxin to promote localization to periplasm and to hexahistadine (His6) to facilitate purification using standard Ni-IMAC chromatography methods, and a carboxyl terminal E-tag for detection. Based on ELISA[8], 10 unique Nbs with 10 nM or better apparent affinities were selected for further analyses (Table S1) (Fig. S6A).

A competition study was conducted to determine whether any of the other unique Nb bound to epitopes not recognized by JTT-B10 by performing replicate dilution ELISAs in which the only variation was that one set of ELISAs contained 20 µg/ml of the JTT-B10 Nb protein as a competitor in which the E-tag detection tag was replaced with a myc tag (Figure S6c). The study identified three Nb families that bind to epitopes not competed by JTT-B10 (Table S1).

L929 cell cytotoxicity assay

Nbs^{TNF} and bacterial supernatants were assessed for their ability to neutralize mTNFα using a TNFα-induced cytotoxicity assay in L929 cells, as previously described[9]. Briefly, 100 µl/well of murine fibroblast L929 cells seeded in 96-well plates (5×10^4 cells/well). After overnight incubation, the culture medium was replaced with serial dilutions of bacterial supernatants or purified Nb prepared in RPMI media containing a final concentration of 1.0 µg/ml actinomycin D and 4 ng/mL murine TNF-α (Biolegend 575204). Plates were then incubated at 37 °C for 24 h after which an MTT assay was performed as per the manufacturer's instructions (Trevigen 4890-25-K). The only mTNFα neutralizing Nb was JTT-B10. (Table S1).

TNBS mouse model of colitis and treatment protocol.

Time points and doses for all treatments and administrations are indicated in the Figures and text. TNBS (Sigma, 92822) was diluted to 20 mg/mL in ethanol (50% v/v) and 100 µl administered via enema by inserting a 3.5 French catheter (Utah Medical Products) 3 cm into

the colon. Bacterial strains were prepared as described and administered via oral gavage or enema. Anti-TNF mAb (BioxCell, clone TN3-19.12) was administered intraperitoneally (i.p.). Mice were euthanized by CO_2 overdose. Upon sacrifice, blood was harvested by cardiac bleed, the GI tracts excised, and colon lengths measured. Blood was collected into serum separator tubes, spun for 5 min at 5000 rpm and serum stored at -20°C. The colon was cut longitudinally, the contents removed and the tissue dissected. Half of the tissue was fixed using 4% paraformaldehyde (PFA) overnight at 4 °C for histology. The other half was homogenized in 1 mL of PBS containing 1x HALT protease inhibitor cocktail (Thermo Scientific) before being centrifuged for 10 min at 20,000 g and the supernatant stored at -20°C for later analysis by ELISA.

Cytokine and Nb ELISAs.

The concentrations of mouse TNFα, IL-10, IL-6 (BioLegend) were quantified by ELISA per the manufacturer's instructions. The anti-Nb ELISA was performed as previously described[9].

Histology.

PFA-fixed colon tissue was transferred to 70% ethanol before processing by routine paraffin embedding, sectioning and H&E staining by the DF/HCC Rodent Histopathology Core. A pathologist (J.N.G.), blinded to experimental parameters, determined colitis scores. Each of the following four histologic parameters were scored as absent (0), mild (1), moderate (2), or severe (3): mononuclear cell infiltration, polymorphonuclear cell infiltration, epithelial hyperplasia, and epithelial injury. The scores for the parameters were summed to generate the cumulative histologic colitis score[10]. The cumulative histologic colitis score was then multiplied by an extent score, indicating the proportion (%) of colon involved by colitis: (1) < 10%; (2) 10%–25%; (3) 25%–50%; (4) > 50%. Images were captured at 10× or 40× magnification with a Nikon Eclipse NI-U and NSI-Element Basic Research software (Nikon).

Statistical analyses.

Statistical analyses were performed using GraphPad Prism v.8.3.0. Data are shown as mean ± SEM as noted. Data were analyzed using a Kruskal-Wallis test with Dunn's multiple correction test or a two-way ANOVA with Tukey's test. A p-value <0.05 was considered statistically significant.

References

1. Schmitz, A.M., Morrison, M.F., Agunwamba, A.O., Nibert, M.L. & Lesser, C.F. Protein interaction platforms: visualization of interacting proteins in yeast. *Nature Methods* **6**, 500-502 (2009).
2. Mou, X., Souter, S., Du, J., Reeves, A.Z. & Lesser, C.F. Synthetic bottom-up approach reveals the complex interplay of Shigella effectors in regulation of epithelial cell death. *Proceedings of the National Academy of Sciences of the United States of America* **115**, 6452-6457 (2018).
3. Kuhlman, T.E. & Cox, E.C. Site-specific chromosomal integration of large synthetic constructs. *Nucleic Acids Res* **38**, e92-e92 (2010).
4. Leong, S.A., Ditta, G.S. & Helinski, D.R. Heme biosynthesis in Rhizobium. Identification of a cloned gene coding for delta-aminolevulinic acid synthetase from Rhizobium meliloti. *Journal of Biological Chemistry* **257**, 8724-8730 (1982).
5. Datsenko, K.A. & Wanner, B.L. One-step inactivation of chromosomal genes in Escherichia coli K-12 using PCR products. *Proceedings of the National Academy of Sciences of the United States of America* **97**, 6640-6645 (2000).
6. Reeves, A.Z. et al. Engineering Escherichia coli into a protein delivery system for mammalian cells. *ACS Synth Biol* **4**, 644-654 (2015).
7. Ernst, N.H., Reeves, A.Z., Ramseyer, J.E. & Lesser, C.F. High-Throughput Screening of Type III Secretion Determinants Reveals a Major Chaperone-Independent Pathway. *mBio* **9** (2018).
8. Jaskiewicz, J.J., Tremblay, J.M., Tzipori, S. & Shoemaker, C.B. Identification and characterization of a new 34 kDa MORN motif-containing sporozoite surface-exposed protein, Cp-P34, unique to Cryptosporidium. *Int J Parasitol* **51**, 761-775 (2021).
9. Baarsch, M.J., Wannemuehler, M.J., Molitor, T.W. & Murtaugh, M.P. Detection of tumor necrosis factor alpha from porcine alveolar macrophages using an L929 fibroblast bioassay. *J Immunol Methods* **140**, 15-22 (1991).
10. Garrett, W.S. et al. Communicable ulcerative colitis induced by T-bet deficiency in the innate immune system. *Cell* **131**, 33-45 (2007).

Supplementary Figure Legends

Figure S1. **Schematic overview and evidence that PROT$_3$EcT-2 assembles a functional T3SA.** The Ipa-Mxi-Spa and Mxi-Spa operons (a) were captured and integrated into the chromosome of *E. coli* resulting in mT3_ Ipa-Mxi-Spa and mT3_Mxi-Spa, respectively (b). The absence of the Ipa operons enables mT3_Mxi-Spa to secrete proteins into its surroundings as opposed to injecting them into host cells. (c) Secretion of OspC2-FLAG by the indicated strains was monitored by a 6 hr liquid secretion assay. Immunoblots of FLAG-tagged OspC2 and GroEL. Data in each panel is representative of results from at least 2 independent experiments. P = whole cell pellet lysates, S = supernatant fractions.

Figure S2. Comparison of secretion of Nb by PROT$_3$EcT and native E. coli carrier proteins. (a) 6 h liquid secretion assays monitoring the secretion of FLAG-tagged NbStx2 dimers fused to designated native E. coli carrier protein sequences in EcN and BL21 E. coli (b). FL = full length CeI-CD. Data in each panel is representative of results from at least 2 independent experiments.

Figure S3. **PROT$_3$EcT-4 stably maintains its alr-plasmid** (a) Plasmid retention rate in strains indicated. Bacterial cultures were back diluted daily for 7 days and grown in LB media without antibiotics. Each day cultures were sampled and plated on LB media to quantify total bacteria and LB/ampicillin plates to quantify bacteria that had retained their plasmid. Data in each panel is representative of results from at least 2 independent experiments. CFU = colony forming units.

Figure S4. **Plate assay of shed bacteria from mice colonized with PROT3EcT-4 and weights of mice treated as indicated.** (a-c) 6 h plate secretion of colonies of PROT3EcT-4 shed from mice at the times indicated. Membranes were removed and probed with an anti-FLAG Ab to monitor Nb secretion. (d) Body weight change (%) of mice inoculated with the strains indicated. Data in each panel is representative of results from at least 2 independent experiments. (b) Data were analyzed using two-way ANOVA with Tukey's post-hoc test. ns = not significant.

Figure S5. **In vitro validation of pMM534 and pMxiE-Lux reporters, and levels of bacteria in mice inoculated with PROT$_3$EcT-3 and treated with antibiotics.** (a,f) Luminescence readings of the strains indicated. Bacteria were grown for 18 h, back diluted 1:100 into plates containing media. At 2 h post back dilution luminescence and OD_{600} were recorded. (b,e) IVIS images of the indicated strains that have been spread on agar plates or grown in liquid culture for 18 h. (d) Schematic of pMxiE-Lux reporter. VirB promotes the expression of MxiE which is activated when bound to IpgC. For these assays, a plasmid that encodes IpgC was introduced into the strains, as is encoded in the Ipa operon, which is absent from PROT$_3$ECT. RLU = relative luminescence units. OD = optical density.

Figure S6. Nb^{TNF} discovery and in vitro testing. (a) Nb^{TNF} DNA sequences. (b) Affinities of purified Nb^{TNF} were measured by ELISA. (c) Functional activity of the Nb^{TNF} was measured using the TNF-L929 killing assay.

Figure S7. TNBS colitis is TNFα dependent. (a) Study design. BALB/c mice were treated with TNBS as before and administered anti-TNFα monoclonal antibody (mAb) intraperitoneally (i.p.) at the times indicated and sacrificed at 5 days post TNBS. (b) Body weight change (%). (c) Colon length. (d) Histologic colitis scores. (e-g) TNFα levels were measured in the indicated samples by ELISA. Data are representative of at least 2 experiments with n=3–5 mice per group and are presented as individual values and mean ± SEM (b) or mean ± SEM (c-g). Data were analyzed using two-way ANOVA with Tukey's post hoc test (b) or a Kruskal-Wallis test with Dunn's multiple correction test (c-g). *, $P < 0.05$; **, $P < 0.01$; ***, $P < 0.001$ denotes comparison to PBS group or as indicated.

Figure S8. **TNF-$PROT_3EcT$ and -T_3EcT-3 are efficacious in the TNBS model when administered via enema.** (a) Study design. BALB/c mice were treated with TNBS as before and administered PBS or an inoculum of 10^8 CFU of T_3EcT-3, TNF-T_3EcT-3, $PROT_3EcT$-4 or TNF-$PROT_3EcT$-4 via enema administration at the times indicated and were sacrificed at 5 days post TNBS. (b) Shed bacteria. (c) Body weight change (%). (d) Colon length. (e) Histologic colitis scores. (f) 6 h liquid secretion assays monitoring the secretion of FLAG-tagged Nb^{TNF} and Nb^{Stx2} by the indicated strains. (g) Plate secretion assay of shed bacteria. Data were combined from 2 independent from at least n = 2 experiments with 3–5 mice per group and are presented as individual values and mean ± SEM (d-e) or mean ± SEM (b-c). Data were analyzed using two-way ANOVA with Tukey's post hoc test (b, c) or a Kruskal-Wallis test with Dunn's multiple correction test (d-e). *, $P < 0.05$; **, $P < 0.01$; ***, $P < 0.001$ denotes comparison to PBS group or as indicated; $^{\#}$, $P < 0.05^{\#\#}$, $P < 0.01$; $^{\#\#\#}$, $P < 0.001$ denotes comparison to $PROT_3EcT$-4.

Figure S9. **Levels of Nb^{TNF} and anti-TNFα mAb in serum, colon tissue and colon contents of treated mice**. Nb^{TNF} levels were measured by ELISA in (a) serum, (b) colon tissue homogenates and (c) colon contents of mice receiving the strains or treatments indicated. Dotted line indicates maximal background in the ELISA. Data were combined from 2 independent experiments.

Figure S1

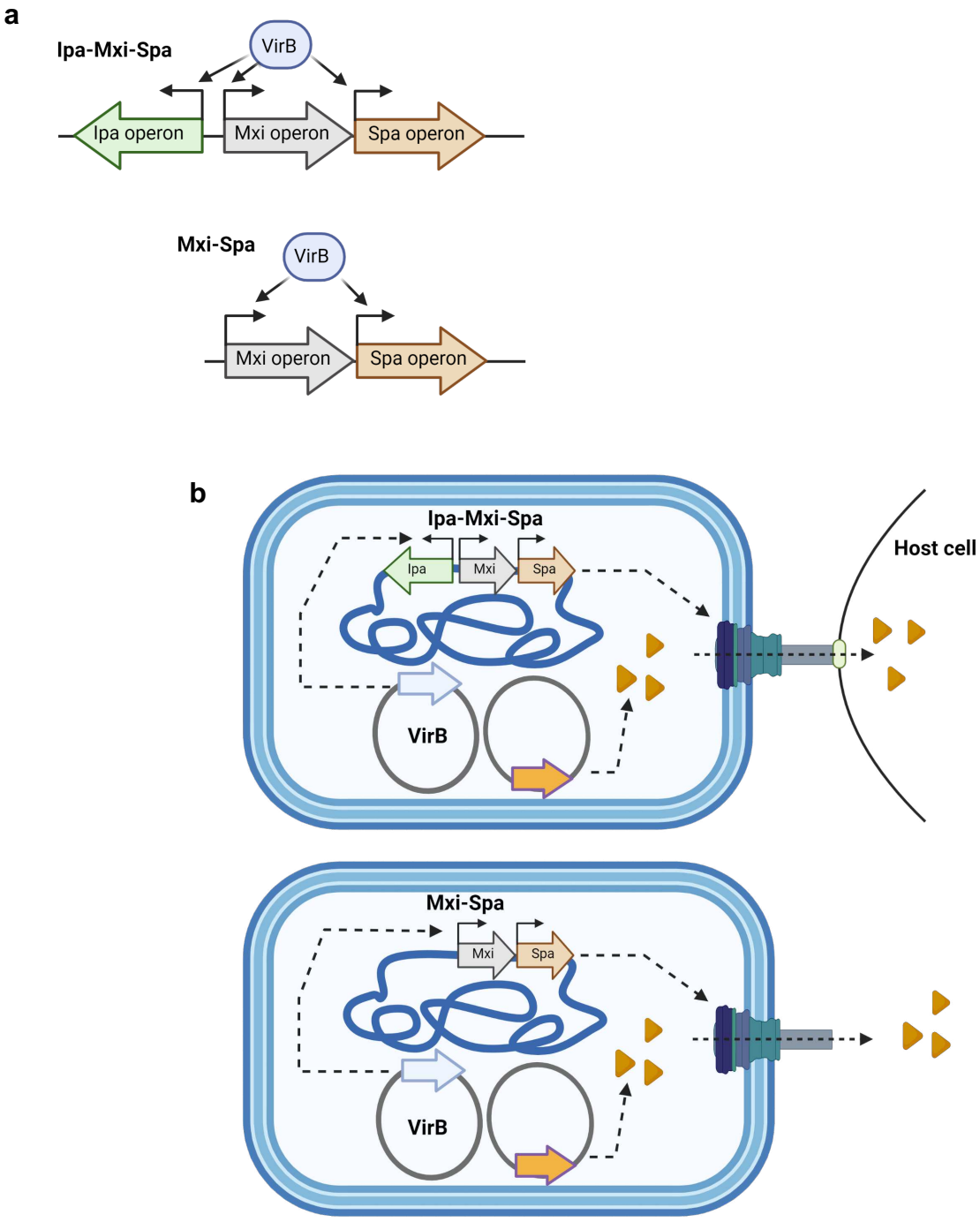
a
Ipa-Mxi-Spa
VirB
Ipa operon
Mxi operon
Spa operon
Mxi-Spa
VirB
Mxi operon
Spa operon
b
Ipa-Mxi-Spa
Ipa
Mxi
Spa
VirB
Host cell
Mxi-Spa
Mxi
Spa
VirB
c
OspC2
GroEL
S
OspC2
GroEL
P
1 2 1 2
PROT3EcT-2
mT3Ec_Mxi-Spa

Figure S2

a

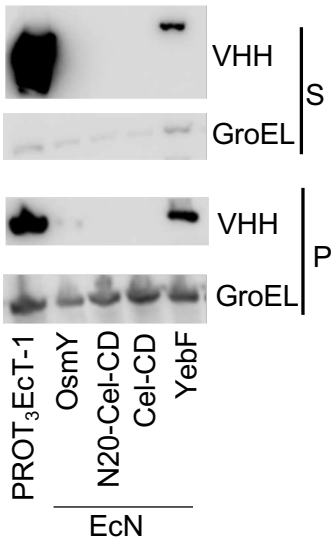
VHH
GroEL
S
VHH
GroEL
P
PROT3EcT-1
OsmY
N20-CelI-CD
CelI-CD
YebF
EcN

b

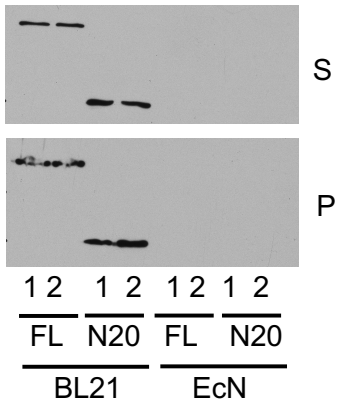
S
P
1 2 1 2 1 2 1 2
FL N20 FL N20
BL21 EcN

Figure S3

a

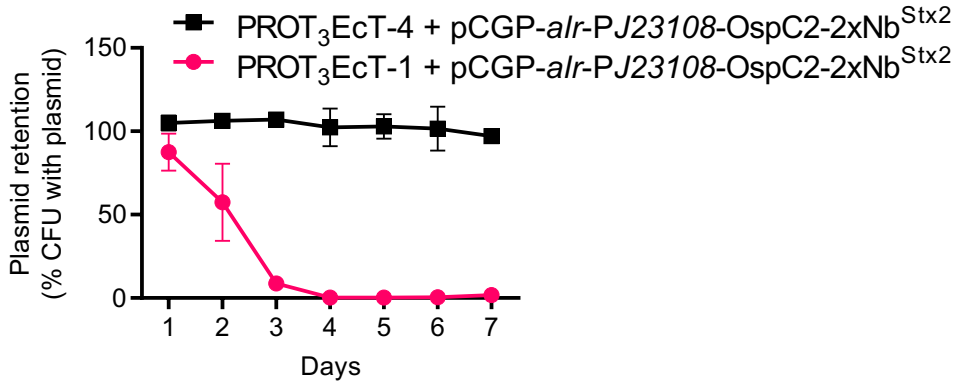
PROT3EcT-4 + pCGP-alr-PJ23108-OspC2-2xNbStx2
PROT3EcT-1 + pCGP-alr-PJ23108-OspC2-2xNbStx2
Plasmid retention
(% CFU with plasmid)
150
100
50
0
1
2
3
4
5
6
7
Days

Figure S4

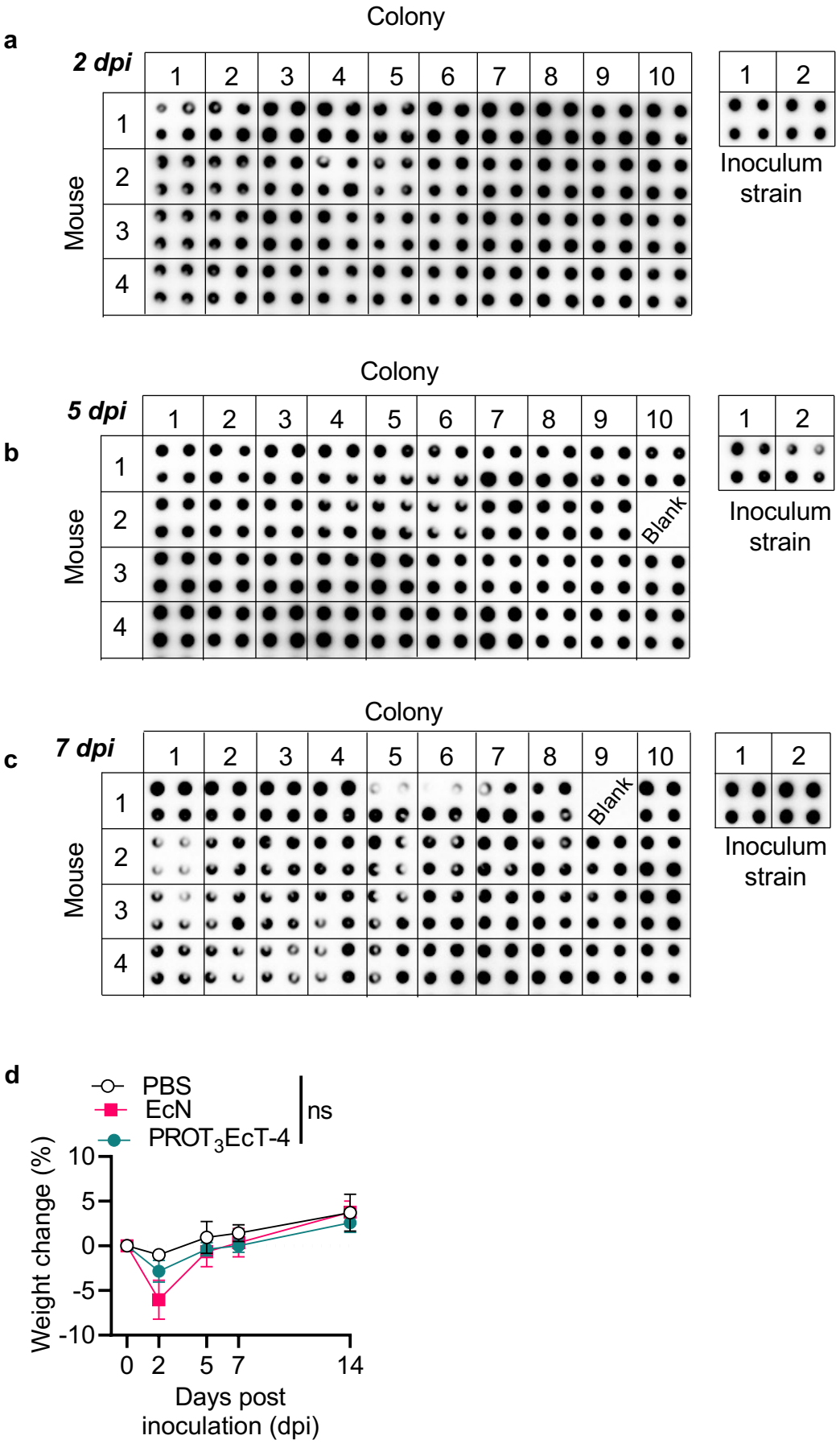
a
2 dpi
Colony
1 2 3 4 5 6 7 8 9 10
Mouse
1
2
3
4
1 2
Inoculum strain
b
5 dpi
Colony
1 2 3 4 5 6 7 8 9 10
Mouse
1
2
3
4
Blank
1 2
Inoculum strain
c
7 dpi
Colony
1 2 3 4 5 6 7 8 9 10
Mouse
1
2
3
4
Blank
1 2
Inoculum strain
d
PBS
EcN
PROT3EcT-4
ns
Weight change (%)
10
5
0
-5
-10
0 2 5 7 14
Days post inoculation (dpi)

Figure S5

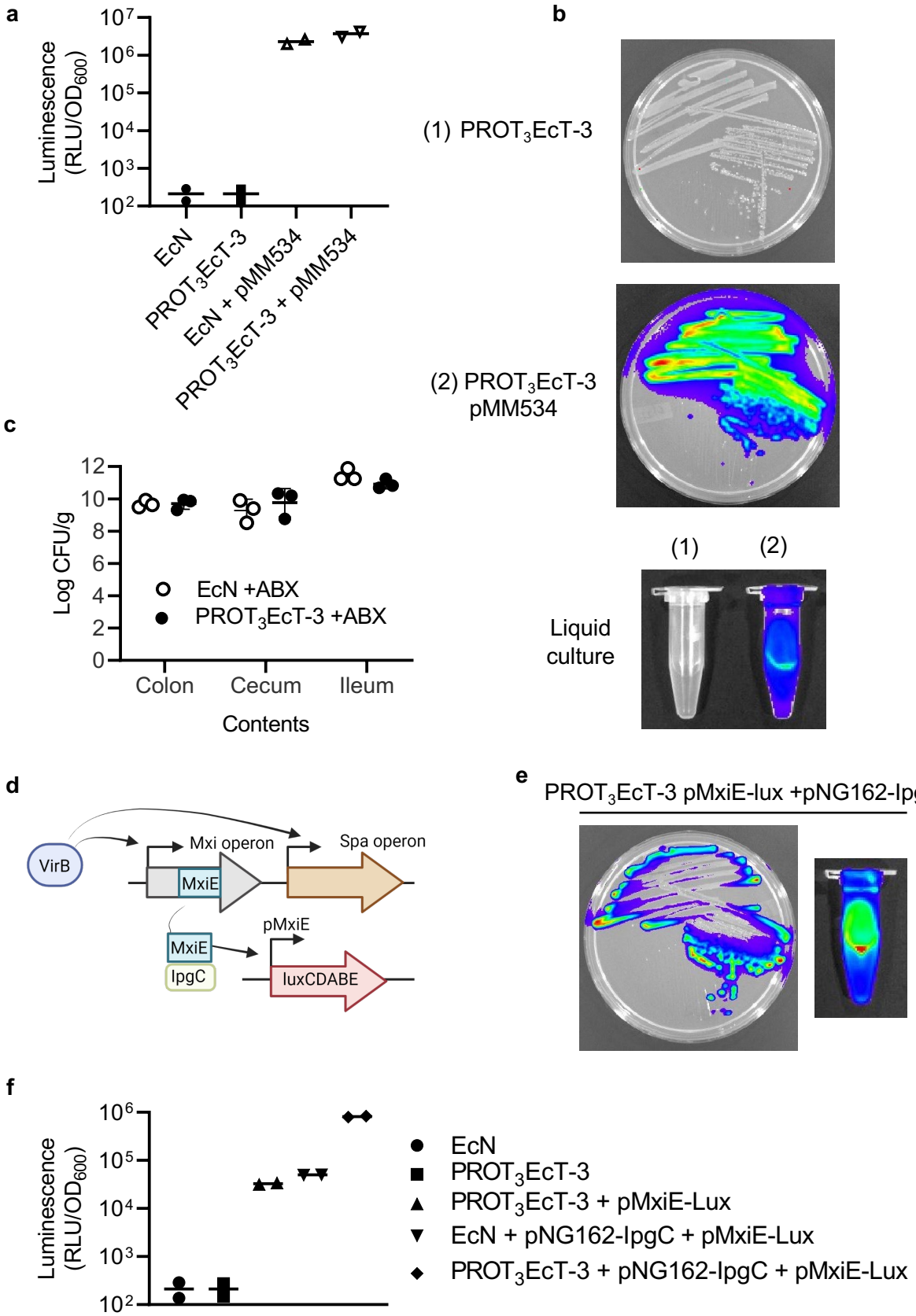
a
Luminescence (RLU/OD600)
EcN
PROT3EcT-3
EcN + pMM534
PROT3EcT-3 + pMM534
b
(1) PROT3EcT-3
(2) PROT3EcT-3 pMM534
(1)
(2)
Liquid culture
c
Log CFU/g
EcN +ABX
PROT3EcT-3 +ABX
Colon
Cecum
Ileum
Contents
d
VirB
Mxi operon
Spa operon
MxiE
pMxiE
MxiE
IpgC
luxCDABE
e
PROT3EcT-3 pMxiE-lux +pNG162-IpgC
f
Luminescence (RLU/OD600)
EcN
PROT3EcT-3
PROT3EcT-3 + pMxiE-Lux
EcN + pNG162-IpgC + pMxiE-Lux
PROT3EcT-3 + pNG162-IpgC + pMxiE-Lux

Figure S6

a

```
                            CDR1                  CDR2                                                  CDR3
NbTNF
JTT-B10   TGGGLVQAGDSLRLSCAASLHFFSTSAMGWFRQAPGKDREFVGVISYGG--GDTEYANSVKGRFTISRDNAKNTVYLQMNSLNPEDTAVYYCVS-------GGYYNIRTGRPTYWGQGTQVTVSS
JUM-E5    SGGGSVQPGGSLKLSCAAHGLT--LDDYGIGWFRQAPGLEREGIACISRSGNAIAYMDSVKGRFTISRDDAKNTVYLQMNSLEPDDTGVYFCAA-GQRIYTVQGRCILYPKTDYWGQGTQVTVSS
JUM-G5    TGGGLVQAGGSLRLSCTVSGRT--FEDTAMGWFRQAPGKEREFVATISWSSGSIYYGETVEGRFTVSRDNAKNTMWLQMNNLKPEDTAVYYCAA-----ARTRYSSRWSSSYDSWGQGTQVTVSS
JUM-G10   TGGGLVQAGDSLRLSCAASGGT--FSTLHVAWFRQAPGKERDFVADISGTGSLTYYTDSVKGRFTISRDNAKNTIYLQMNSLKPEDTAVYYCAG------NRGYGFRTSNRFDYWGQGTQVTVSS
JUN-A1    TGGGLVQAGDSLNITCVASGRT--FKNVAMGWFRQAPGKEREFVAAISWHGGNTVYADSVKGRFAITRNNAKDALYLQMRSLKAEDTAVYYCAQ-------GNYYALQTGRSDYGGQGTQVTVSP
JUN-B9    TGGGLVQPGGSLTLSCAASGFS--FSTFYMSWLRQAPGKGLEWVAEISPISSTADYADSVKDRFTLSRDNSENTLTLQMSSLKPEDTAVYYCAP----------GSRAVALRNSRGPGTQVTVSS
JUN-C12   TGGGLVQAGGSLRLSCAASGRT--FSDYAMGWFRQVPGKEREFVAAINWSGRSTWYADAVRGRFTISRDDAKNTVFLQMNRLKLEDTAVYYCAA-----GQGPEIWTTASRFVSWGQGLQVTVSS
JUN-F5    SGGGLVQAGGSLRLSCAASLRF--FSESSMGWFRQAPGKEREFVASISRSGGDTNYADSVKGRFTISRDNAKNMVFLQMNSLKPEDTAVYYCAG----SSSYYRLSYYPNLSDYWGQGTQVTVSS
JUN-G4    SGGGLVQPGGSLRLSCAASGFT--FSISAMAWYRQTPENGREWVATISS-RGATNYADSVKGRFTISRDSG---LYLQMNNLKPEDTAVYYCNT-------------NPPMFRSWGQGTQVTVSS
JUN-G10   SGGGLVQAGGSLRLSCAASGRF--FSSVAMGWFRQAPGKERELVAAISWSGGDTSYADSVKGRFTISRDNSKNMVYLQMNSLKPEDTAVYYCAR------HGSYYSLLTESVDYWGQGTQVTVSS
JUN-H5    SGGGLVQAGGSLRLSCAASGRD--FSGYTMAWFRQAPGKEREFVAANSWSGGSTYYTGSVKGRFTISRDNAKNMVYLQMNSLRPEDTAVYYCAA------GPHRTSDSVKGYDFWGQGTQVTVSS
```

b

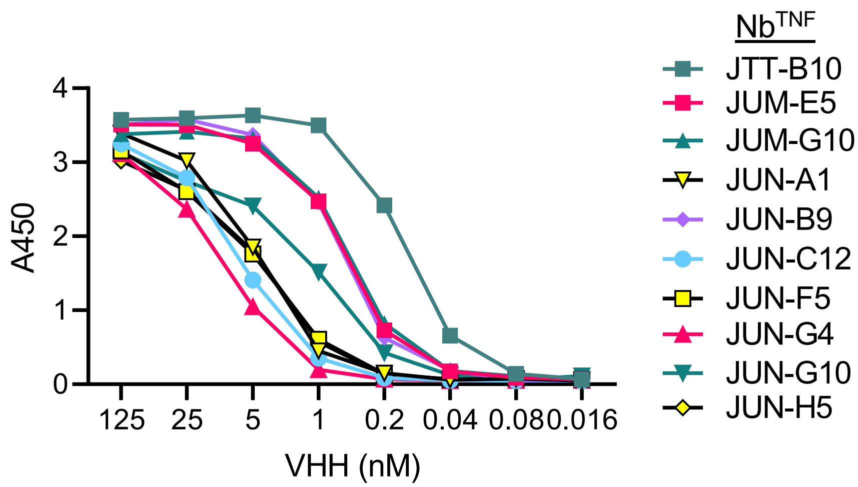

c

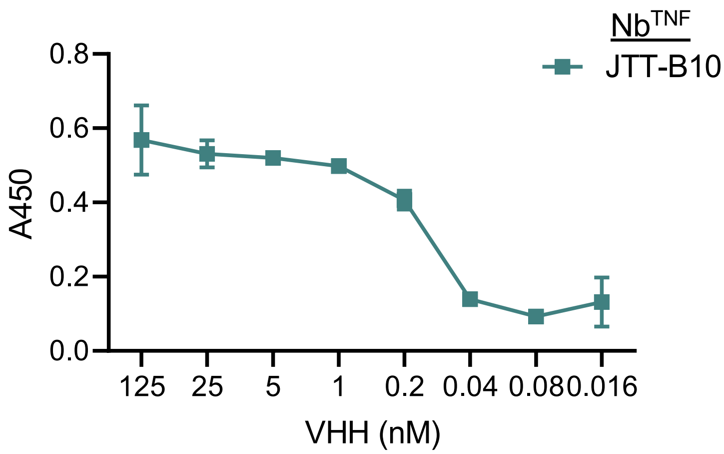

Figure S7

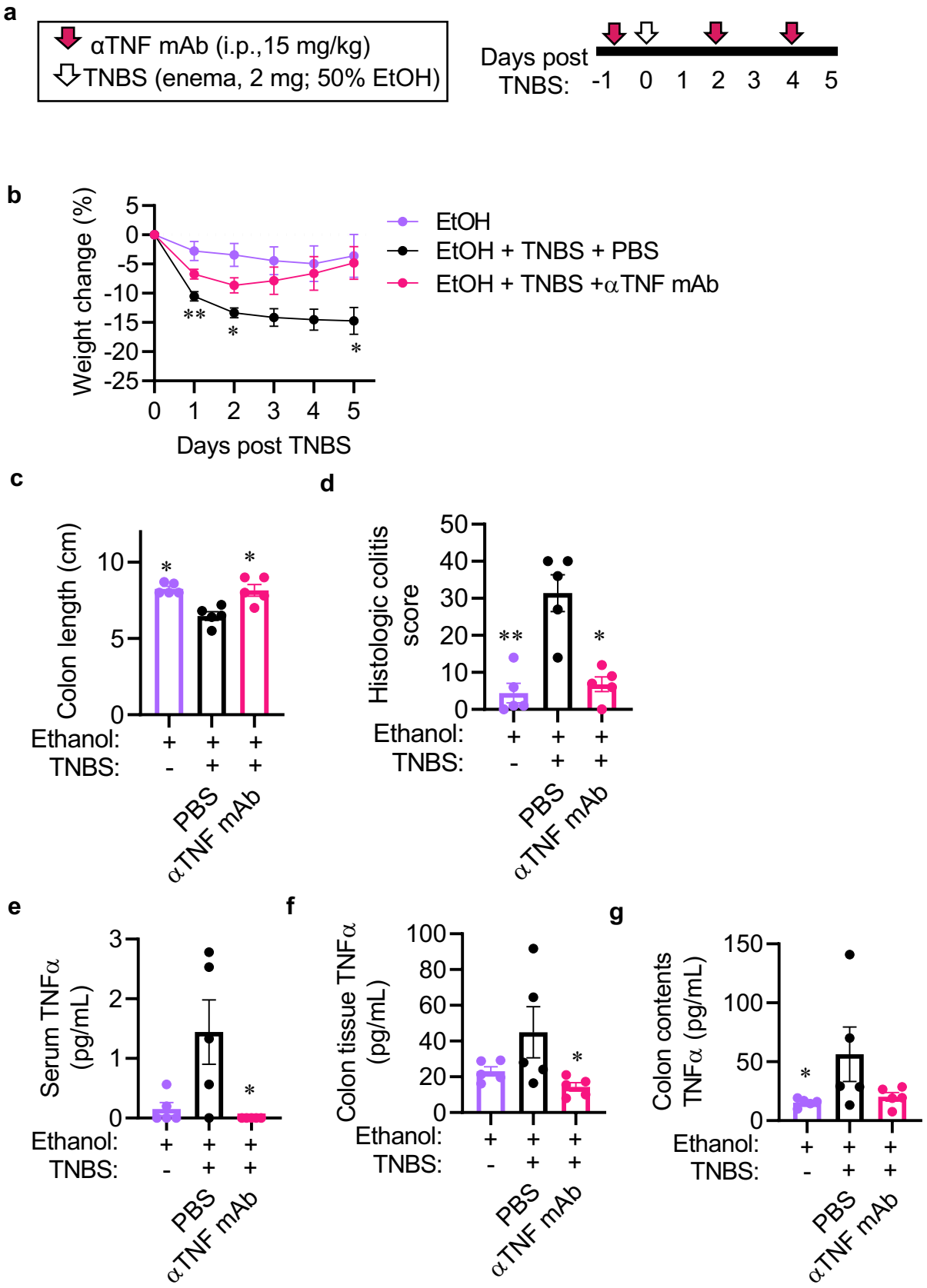
a
αTNF mAb (i.p.,15 mg/kg)
TNBS (enema, 2 mg; 50% EtOH)
Days post TNBS:
-1 0 1 2 3 4 5
b
Weight change (%)
Days post TNBS
EtOH
EtOH + TNBS + PBS
EtOH + TNBS +αTNF mAb
c
Colon length (cm)
d
Histologic colitis score
Ethanol:
TNBS:
PBS
αTNF mAb
e
Serum TNFα (pg/mL)
f
Colon tissue TNFα (pg/mL)
g
Colon contents TNFα (pg/mL)

Figure S8

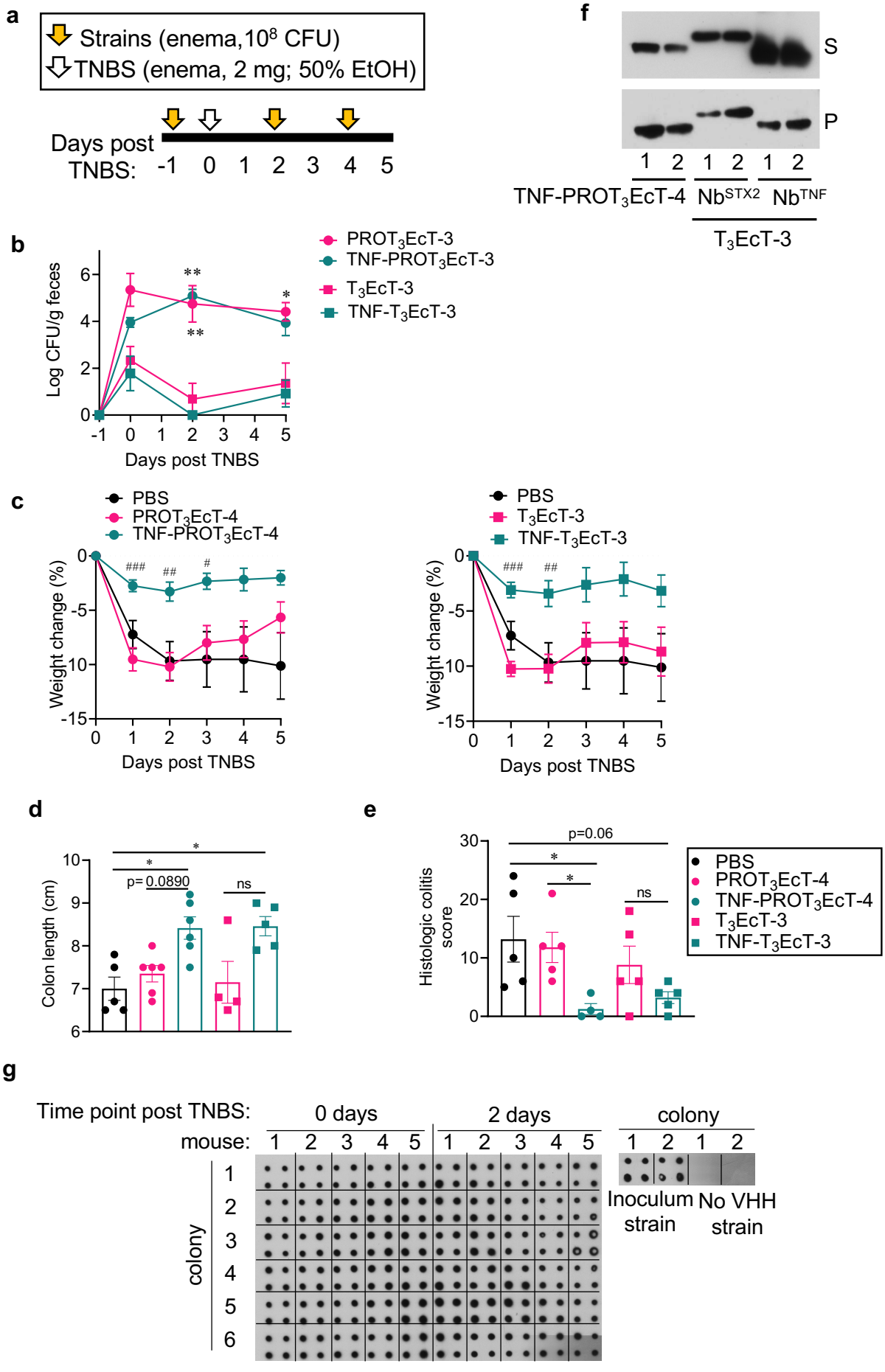
a
Strains (enema,10^8 CFU)
TNBS (enema, 2 mg; 50% EtOH)
Days post TNBS: -1 0 1 2 3 4 5
f
S
P
1 2 1 2 1 2
TNF-PROT3EcT-4 NbSTX2 NbTNF
T3EcT-3
b
PROT3EcT-3
TNF-PROT3EcT-3
T3EcT-3
TNF-T3EcT-3
Log CFU/g feces
Days post TNBS
c
PBS
PROT3EcT-4
TNF-PROT3EcT-4
Weight change (%)
Days post TNBS
PBS
T3EcT-3
TNF-T3EcT-3
Weight change (%)
Days post TNBS
d
Colon length (cm)
p= 0.0890
ns
e
Histologic colitis score
p=0.06
ns
PBS
PROT3EcT-4
TNF-PROT3EcT-4
T3EcT-3
TNF-T3EcT-3
g
Time point post TNBS:
0 days
2 days
colony
mouse:
1 2 3 4 5 1 2 3 4 5 1 2 1 2
colony
1 2 3 4 5 6
Inoculum strain
No VHH strain

Figure S9

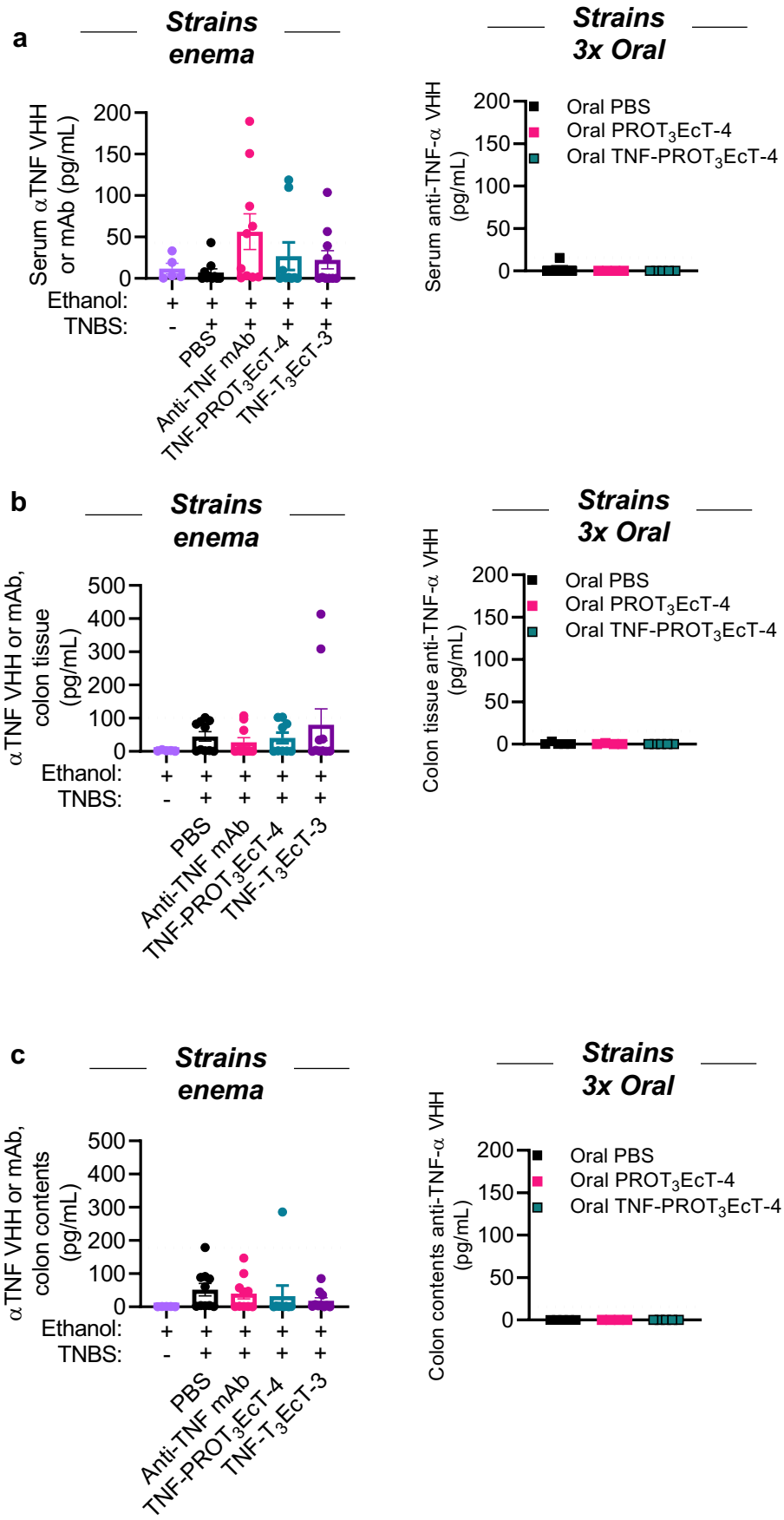
a
Strains
enema
Serum αTNF VHH or mAb (pg/mL)
200
150
100
50
0
Ethanol: + + + + +
TNBS: - + + + +
PBS
Anti-TNF mAb
TNF-PROT3EcT-4
TNF-T3EcT-3
Strains
3x Oral
Serum anti-TNF-α VHH (pg/mL)
Oral PBS
Oral PROT3EcT-4
Oral TNF-PROT3EcT-4
b
Strains
enema
αTNF VHH or mAb, colon tissue (pg/mL)
500
400
300
200
100
0
Ethanol: + + + + +
TNBS: - + + + +
PBS
Anti-TNF mAb
TNF-PROT3EcT-4
TNF-T3EcT-3
Strains
3x Oral
Colon tissue anti-TNF-α VHH (pg/mL)
Oral PBS
Oral PROT3EcT-4
Oral TNF-PROT3EcT-4
c
Strains
enema
αTNF VHH or mAb, colon contents (pg/mL)
500
400
300
200
100
0
Ethanol: + + + + +
TNBS: - + + + +
PBS
Anti-TNF mAb
TNF-PROT3EcT-4
TNF-T3EcT-3
Strains
3x Oral
Colon contents anti-TNF-α VHH (pg/mL)
Oral PBS
Oral PROT3EcT-4
Oral TNF-PROT3EcT-4